Hugo Paisana

Hydrographics Electronics: Functionalize any 3D Surface

Dissertação de Mestrado em Engenharia Eletrotécnica e de Computadores
09/2017

· U C ·

UNIVERSIDADE DE COIMBRA

Hydrographics Electronics: Functionalize any 3D Surface

Hugo Paisana

Supervisor:
Prof. Doctor Mahmoud Tavakoli

Jury:
Prof. Doctor Mahmoud Tavakoli
Prof. Doctor Maria do Carmo Medeiros
Prof. Doctor Mário João Ferreira dos Santos

Dissertation submitted to the Electrical and Computer Engineering Department of the Faculty of Science and Technology of the University of Coimbra in partial fulfilment of the requirements for the Degree of Master of Science.

Coimbra, September of 2017

Acknowledgements

Nem sempre nesta caminhada tudo correu como o pretendido. É, no entanto, com estes pequenos obstáculos que uma pessoa cresce a aprende.

Gostava de agradecer em primeiro lugar aos meus pais, irmã e avós. Não só por suportarem os meus custos no ensino superior durante estes anos, mas também por todo o apoio, carinho e conselhos dados.

Um obrigado a todos os meus colegas e amigos de curso por todas as vivências, partilhas e ajudas que me deram durante este percurso difícil.

Quero também agradecer a todos os meus colegas que me apoiaram e muito me ajudaram este último ano no ISR onde concluí a minha dissertação. Ao Professor Mahmoud Tavakoli que acreditou nas minhas capacidades de desenvolver tal projeto e me permitir evoluir imenso.

Um obrigado a todos,
Hugo Paisana

Abstract

A novel method for fabrication and transfer of printed circuits is introduced. This method allows digital printing of conductive traces over various surfaces, including tattoo paper and water transfer paper. In addition, a novel material composition and process is introduced for fabrication of such circuits (pro-visionary US Patent filed).

Moreover, and inspired from children temporary tattoos, we produced circuits that can be transferred over the human body for bio-monitoring through measurement of bio-potentials over the epidermis layer of the human skin. As a case study, we show an electromyography (EMG) electrodes transferred over a volunteer skin which allows human hand gesture recognition through monitoring of the forearm muscles.

Also inspired from the hydro-graphics printing technique, we showed circuits that can be transferred on three dimensional shapes. Hydro-graphics printing is recently becoming a popular method for transferring graphics over various parts, specially for car aesthetics. Here, we showed how electronics circuits can be transferred to such parts. As case study two circuits were presented, a headphone part was activated with touch buttons to control music volume and a 3D printed back-shell of a prosthetic hand was also updated with tactile buttons as human input and a RGB LED as the human interface.

The process, material composition and results are presented in this dissertation.

Keywords: **Ink-Jet Printing, Hydro-Transfer, Conductive Circuits, Stretchable Electronics, Liquid Metal, Silver Nano-Particle Ink**

"If you can’t do great things, do small things in a great way." - Napoleon Hill

Resumo

Um novo método de fabricação e transferência de circuitos impressos é introduzido. Este método permite a impressão digital de caminhos condutores sobre vários tipos de superfícies, incluindo papel de tatuagem e papel de transferência de água. Além disso, são introduzidos novos tipos de materiais e processos para a fabricação de tais circuitos (patente nos EUA preenchida).

Para além disso, e inspirado em tatuagens temporárias para crianças, conseguimos produzir circuitos que podem ser transferidos para o corpo humano com o objectivo de bio-monitorização através de bio-substâncias encontradas na pele humana. Como estudo de caso, mostramos eléctrodos eletromiográficos (EMG) transferidos sobre pele humana e que permitem o reconhecimento do gesto das mãos humanas através da monitorização dos músculos do antebraço.

Também inspirados na técnica de impressão hidro-gráfica, mostramos que circuitos podem ser transferidos para objectos com formas tridimensionais. A impressão hidro-gráfica está a tornar-se um método popular para transferir gráficos em várias partes e superfícies, especialmente para melhorar a estética de automóveis. Mostramos como circuitos eléctricos podem ser transferidos para essas mesmas partes e superfícies. No estudo de caso, dois circuitos foram apresentados, uma parte de um headphone que é activada ao pressionar botões impressos para controlar o volume da música, e uma peça para uma mão robótica foi actualizada com botões impressos e um LED RGB como interface para o controlo da mesma.

O processo, a composição do material e os resultados são apresentados nesta dissertação.

Palavras chave: **Impressão Ink-Jet, Impressão Hidro-Gráfica, Circuitos Condutores, Deformável, Metal Liquido, Tinta de Prata**

List of acronyms

HRI Human Robot Interfaces

MEM Micro-Electro-Mechanical System

SI Silver Ink

Au Gold

Ag Silver

NP Nano-Particle

LM Liquid Metal

ET Electronic Tattoo

PVA Polyvinyl Alcohol

AgNP Silver Nano-Particle

EGaIn Eutectic Gallium-Indium

TTP Temporary Tattoo Paper

AAS Acetic Acid Solution

CSPP Conductive Silver Polymer Paste

SEM Scanning Electron Microscopy

TP Tracing Paper

Table of contents

List of acronyms **ix**

List of figures **xiii**

List of tables **xvii**

1 Introduction **1**
1.1 Motivation and Overall Goals 4
1.2 Structure of Dissertation 6

2 State of the Art **7**
2.1 Contributions 13

3 Materials, Methods and Results **15**
3.1 Materials 15
3.1.1 Substrates 15
3.1.2 Printer and Cartridges 17
3.1.3 Inks 19
3.1.4 Conductive Silver Polymer Paste 20
3.1.5 Liquid Metal 20
3.1.6 Acetic Acid Solution and HCL Vapour 21
3.2 Methods 22
3.3 Results 31
3.3.1 Conductivity 31
3.3.2 Strain Tests 33
3.3.3 SEM Microscopy 37
3.4 Conclusion 42

4 Case Studies **43**
4.0.1 Capacitive 3D Printed Hand Piece 43
4.0.2 Capacitive Multi-Layer Keyboard 48
4.0.3 Headphone with integrated capacitive bottoms 49
4.0.4 EMG Reader Tattoo 51

5 Future Work and Publications **54**
5.0.1 Future Work 54
5.0.2 Publications 55

References **56**

List of figures

1.1 Digital clock in a wearable ring [1]. 1
1.2 Wearable electronics' technological branches. 2
1.3 Forecasted value of the global wearable devices market from 2012 to 2018 [2]. 3
1.4 Printed AgNP ink circuit with micro-electronics. 5

2.1 Characteristic properties and diverse functions or applications of recently developed devices for E-skins [3]. 8
2.2 Sweat-Monitoring device [4]. 9
2.3 (A) Temperature sensing tattoo, (B) Close-up of temperature sensing tattoo, showing heating wire and Au wires encapsulated with polyimide, (C) Side-schematic of the tattoo, (D) Thermal snapshot of the tattoo on skin, (E) Temperature changing graphic generated over time. 10
2.4 Bio-stamp temporary wireless antenna tattoo. 10
2.5 (A) Thermal print-head, (B) Piezoelectric print-head. 12
2.6 How AgNP Ink obtains conductivity [5]. 13

3.1 (A) TTP layers being separated (white paper removed refers to the protective back layer, transparent film with the drawn pattern to the transferable film), (B) Side Schematic. 16
3.2 (A) PVAc with printed design is placed on the surface of a container filled with water, (B) After the PVAc emulsion has finished when reacting with water, the pattern can be transferred to the desired surface, in this case, a automotive piece, (C) The final result after drying for a few hours at room temperature. 17
3.3 Modified HP840C Printer 18
3.4 (A) Removing the outside case, (B) Side view, showing the laser encoder and paper feed motor, (C) Rear view, showing the paper feed gears and the second paper feed roller, now removed. 18

3.5 C6615 Series cartridge without side cover and open. 19
3.6 Silver Nano-Particle ink printed circuit. 20
3.7 Liquid Metal deposition due to oxide layer. 21
3.8 Phases required to make a conductive circuit with Ag and LM. 23
3.9 Printing a circuit with AgNP Ink. 23
3.10 (A) Deposition of LM over the substrate, (B) Spreading the LM, (C) LM spread over all the substrate. 24
3.11 (A) Applying the acidic solution, (B) Cleaned substrate. 24
3.12 Placing a small LED on the circuit using a pincer. 25
3.13 IC Chip fixed in a PCB using silver paste. 26
3.14 (A) Immersed 3D printed Mouse Piece with TTP film floating above, (B) 3D printed Mouse Piece grabbing the TTP film into its surface, (C) Final result. 26
3.15 Host surface submerged in the water container and floating TTP above. . . 27
3.16 3D Printed piece with a conductive TTP circuit curving around the surface. 28
3.17 (A) Tattoo Transfer Paper applied directly on the skin with protective back layer, (B) Tattoo Transfer Paper fixed on the skin with protective back layer removed. 28
3.18 Polyvinyl acetate composing layers. 29
3.19 (A) Removing PVAc protective back layer by hand, (B) PVAc forming wrinkles due to the reaction with water, (C) Transferring the PVAc circuit to the host surface, from above. 30
3.20 Tracing Paper with conductive lines. 31
3.21 180º Turn close up in a 3D printed piece, using TTP. 33
3.22 Some of the samples used in the strain tests. 34
3.23 Sandwich method explained. (A) Bottom cured PDMS layer, (B) TTP film transferred to the bottom PDMS layer, (C) Encapsulating top PDMS layer. . 34
3.24 Device used to stretch the line samples. 35
3.25 Result of one sample test. Orange trace represents the average resistance and the red trace the distance travelled (40*mm*) from the original position on each repetition cycle. 36
3.26 Breakpoint test results for one sample tested (continuous orange line) and orange dots representing the breakpoint for the remaining samples. 37
3.27 (A,C,E,G) AgNP printed trace on TTP before alloying LM at different magnifications, (B,D,F,H) Final result after alloying and cleaning the AgNP printed traces with LM at different magnifications with AAS. 38

3.28 (A) BSE scan on the sample surface showing the frontier between AgNP (blue) printed ink and the substrate (red), (B) Elemental Analysis through Energy-Dispersive X-Ray Spectroscopy, showing in red the substrate and in blue the Ag element, (C) Percentage of each element in the scan performed 40
3.29 (A) SEM Microscopy performed reveals bright and grey zones at 1kx magnitude, (B),(C),(D) Elemental analysis with different types of elements selected, (E) Elemental percentage analysis for grey zones, (F) Elemental percentage analysis for bright zones. 41

4.1 3D printed piece to fit in a robotic prosthetic hand. 44
4.2 Printed circuit schematic on TTP. 44
4.3 (A) Placing drops of EGaIn LM on TTP, (B) Rubbing and applying pressure with a soft paper, (C) Final result. LM distributed over TTP. 45
4.4 (A) Cleaning the surplus LM over the substrate using an AAS, (B) Final result after cleaning and drying the substrate. 45
4.5 (A) TTP with printed circuit and LED floating in the water. The host piece is submerged, (B) Protective back layer from TTP detaching, (C) Attaching the TTP film to the host piece. 46
4.6 Final result after transferring the TTP film to the host piece, showing the front and back respectively. 47
4.7 (A) Back part of the hand piece with connected wires using CSPP, (B) Front part of the hand piece after applying the protective plastic spray. 47
4.8 Robotic Hand grasping an object using the capacitive bottom. 48
4.9 Capacitive Keyboard with 32 intersections and 2 independent bottoms for Space and Enter. 49
4.10 Capacitive headphone. User pressing "On" bottom to turn the device on, turning the red LED active. 50
4.11 Capacitive headphone bottoms with conductive traces bending to the inside part of the headphone case. 50
4.12 Printed EMG electrode on TTP substrate, alloyed with LM and cleaned, with three wires attached for readings. 51
4.13 Printed EMG electrode on TTP substrate connected to the EMG signal reading device. 52
4.14 (A) Watering the protective back layer of the TTP, (B) Peeling off the protective back layer, leaving the electrode exposed due to the film transparency. . 53
4.15 Software recording data as hand is closed for some seconds. 53

List of tables

3.1 Average resistance change for lines of $40mm \times 1.5mm$ over different substrates and with different cleaning methods. 32

Chapter 1

Introduction

Decades, and even centuries ago, people started to use the beginning of wearable technology such as simple watches and such props to improve the human life in general. An example of this evolution is a timing device. Only state buildings had timing devices. The technological progress made it possible for a carriage clock to become a pocket watch, and a few years later, a wristwatch. Today, we achieve a point where this timing device is built into items as small as rings or accessories.

Fig. 1.1 Digital clock in a wearable ring [1].

A wearable is a device related to the generation, modulation and transmission of data, usually obtained via environmental sensors, physiological function sensors, antennas, global-positioning-systems receivers, cameras and sound sensors. As this happens, an interface is a suitable medium to exchange data between devices and the user, as well as between the user and the outside environment [6].

A wearable electronic has a system configuration divided in five main parts: *Interface*, *Communication*, *Energy Supply*, *Data Management* and *Integrated Circuits*. They all have an important role to make a wearable device reliable and functional.

If one of these branches stagnate in technological matters, developing new and better wearable devices is slowed down (e.g. a wearable device that requires a huge amount of energy can't be powered using a car's battery, since the user would have to carry it around).

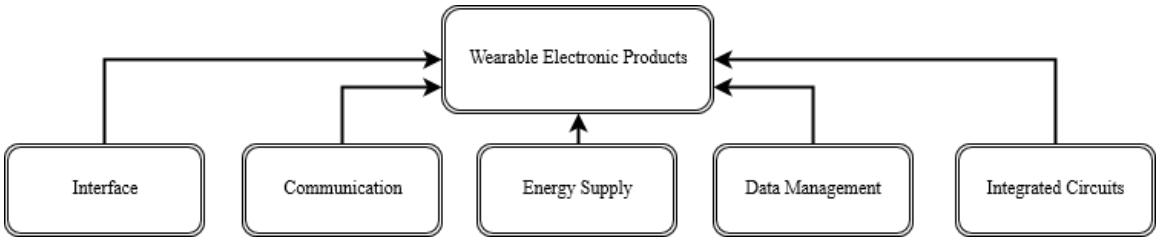

Fig. 1.2 Wearable electronics' technological branches.

With the advancement of wearable technology, stretchable electronics have made a way into being the building blocks of the wearable human machine interfaces of the future. Flexible and stretchable electronics started almost 20 years ago with the demand of macro-electronics [7] [8] [9], such as paper-like flexible displays [10] [11], finding their main destined applications in the late 2000s when the concept of bio-integrated electronics was proposed [12], as epidermal electronics for vital sign monitoring [13] [14], brain computer interfaces [15], electrocardiogram mapping devices [16], and small or minimally invasive surgical [17].

One of the ultimate modern goals in wearable devices is their seamless interfacing with the human user, the envision of revolutionary versions of wearables that are ultra-thin and comfortable, not only for humans but robotic devices. Futuristic wearables are seen as a form of second skin over the human skin (e.g. in the form of an electronic tattoo embedded or bonded over the human epidermis).

Increasing the HRI with better sense and stimulus is now becoming a reality due to the progresses made in second-skin prototypes called electronic skin, or E-skin. Electronic skin by definition is a thin material that contains electrical components which acts like a real or very similar skin [18]. Things human skin can do such as sensing temperature, pressure and stretch are main ambitions when producing E-Skins, as *Kimberly Hoofman et al* [18], recently developed.

With the production of E-skins, robotic devices can be equipped with human-like skin to sense the mechanical and thermal stimuli from the surrounding environments, increasing the HRI when transmitting the received information to human users.

Directly joinning components in stretchable electronics, including E-skins [19], also reduce the need of several wire harnesses and processor boxes attached, minimizing the space and time required to reallocate or placing them in various applications.

Nowadays, wearable and stretchable technology is more than just niche market, it is everywhere with infinite application possibilities. This market reached a value of 300 billion of dollars around the globe in 2017 [20], with a prevision of increasing exponentially to 411.85 billion by 2023 [21], Fig. 1.3, making this an area of interest for various applications.

Most of the investing companies' objectives is to facilitate the daily routine by introducing devices that the user can carry with ease – smart-watches, fitness trackers, smart eye-wear, smart clothing, medical devices – and, recently, the creation and innovation of electronic skins.

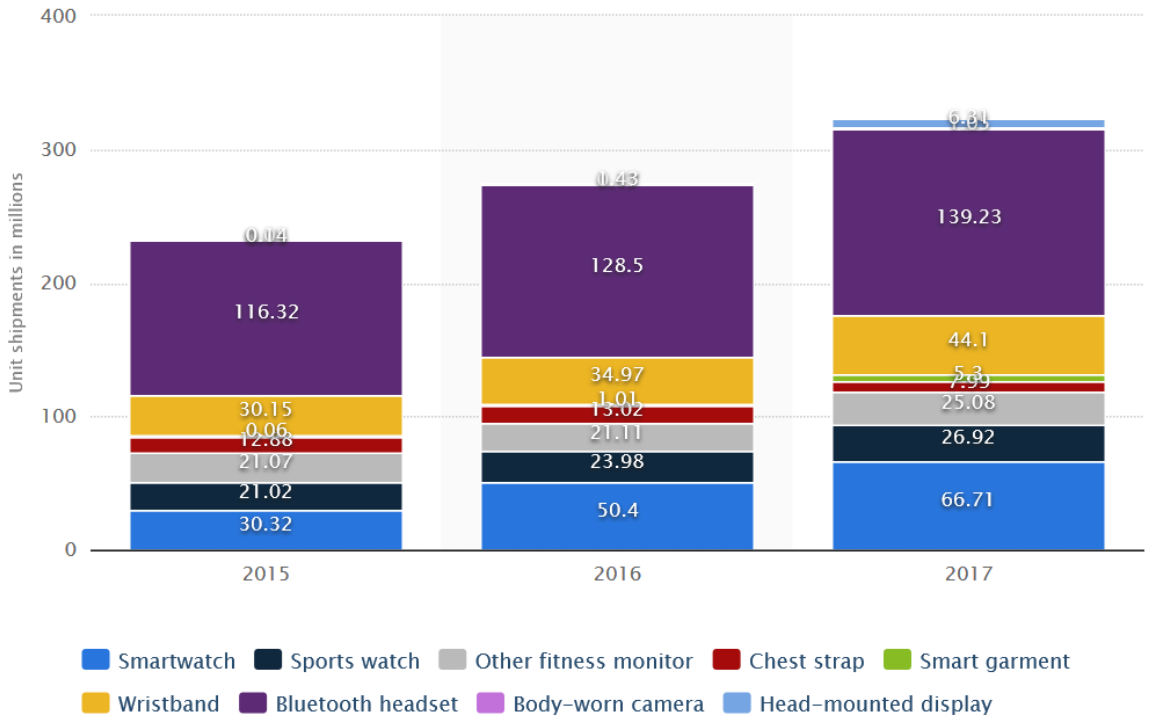

Fig. 1.3 Forecasted value of the global wearable devices market from 2012 to 2018 [2].

Stretchable electronics and E-skins created a footprint in the medical area, from blood glucose sensors, drug delivery and compliance monitoring systems to ophthalmic applications, such as intra-ocular pressure sensors, [22] and sweat analysers [4]. It also made a step into consumer electronics, home electronics and mainly in robotic applications.

Fashion and leisure's market is a growing area when it comes to stretchable electronics too. Customizable wearable and stretchable technology used in smart clothing [23] give the user the feeling of self-identity. It is now being improved in a way from being just a fashion trinket to a user's aid, such as reminders, via vibrating, lights or temperature adjustments.

With the great impact of technology advancements, it is expected that wearable technology will influence our society and culture, as well as our lifestyle. Wearable electronics will have a profound influence on the future development, research and education. Future children will less depend on abilities such as writing, reading and drawing when in an environment where technology offers a much easier way to communicate and perform several tasks.

Having stretchable electronics surfaced recently, a wide quantity of the materials and fabrication methods available aren't totally reliable since there is no specific ways of doing it right yet. This poses a risk of failure due to external variables that may influence the outcome, mostly on human-robot interaction applications (HRI). Many fabrication progresses have been made in the flexible and stretchable electronic skins researches, including laser patterning, micro-contact printing and stencil lithography. Most of those applications depend on the human exact repetition, which is impossible precisely due to the human factor.

Such methods are yet labour intensive and often require expensive materials and processes, from precise sintering methods to nano-working tools and micro-transfer printing [24].

1.1 Motivation and Overall Goals

Circuits that are mechanically robust and compatible with soft biological tissue are central to a broad range of applications, from 3D conformable touch panels to "second-skin" electronic tattoos.

Seminal efforts have focused on deterministic circuit architectures in which stretchable functionality is achieved with circuit traces that have a wavy serpentine geometry [25]. In contrast to ultra-thin plastic electronics [26], which are highly flexible but not stretchable, deterministically-patterned circuits can be transferred to non-developable 3D shapes or bond directly to the skin without constraining natural motion. These approaches rely on clean-room lithography or specialized processing steps that are difficult to perform with low-cost printing or rapid prototyping.

Recently, there has been a growing interest in thin-film stretchable circuits that can be produced with ink-jet printing using common home printers [27], screen printing and other patterning techniques that are rapid and inexpensive. This includes efforts with Au foils [28],

carbon ink and greases [29], conductive polymers like PEDOT:PSS [30], Ag-based inks and elastomer composites [31][32].

In recent times, nano-particle inks have become popular due to their compatibility with regular ink-jet printers. While most of them require some processes to become conductive, sinter-free AgNP inks are particular interesting since they do not require such processes as heating, plasma treatments and other post-processing steps that could damage sensitive circuits and micro-electronics.

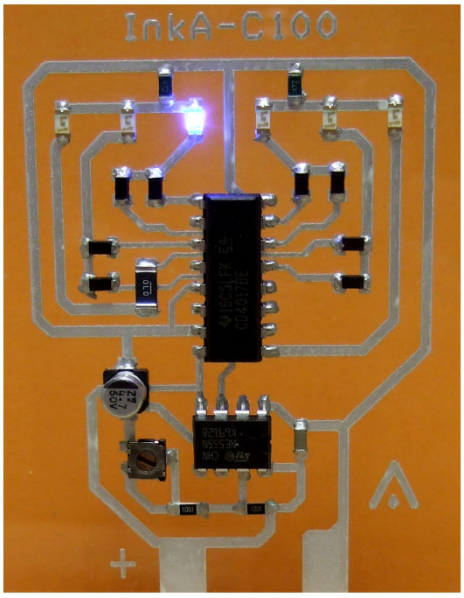

Fig. 1.4 Printed AgNP ink circuit with micro-electronics.

Efforts to develop thinner, soft and flexible electronics are made everyday to change the way we interact with machines. A device must provide comfort if being regularly used, and that is why a search for a much more intimate integration with the body is desired, such as mounting something closely to the skin [33]. Made of a material that can stand up to twisting, pulling without breaking, and poking, but also being stretchable and flexible, electronic tattoos are now being studied for future prototypes on wearable devices.

The goal of this work is then set to suggest an easy method of fabrication of stretchable electronics system with the help of digital printing. The current methods of fabrication of stretchable electronics often require access to clean room facilities and labour intensive processes. The motivation behind this dissertation is to use ink-jet printing as the main fabrication tool for printed electronics. While, there already exist conductive inks for ink-jet printers, they often requires high temperature sintering process, or they work only over a limited number of substrates. Using printer inks over transfer paper has not been previously reported, mainly due to limitations of the inks. In addition, high curing temperatures are not

compatible with transfer paper. But if one is able to print functional circuits over transfer paper, it is then possible to transfer that circuit to any surface including the human body.

This includes an important update on the state of the art to printed electronic systems, and allows printer inks to be applied over a wide range of materials previously not possible. This opens a new door for transferring printed electronics to a wide range of daily objects as well as human organs, namely skin, heart and brain tissues.

1.2 Structure of Dissertation

This dissertation is divided into five main chapters and their related subsections.

The first chapter, *Introduction*, presents the framework, motivation and dissertation's structure. A second chapter, *State of the Art*, summarizes the most common technologies and researches in wearable, stretchable electronics and electronic skins. An exposition of different type of electronic skins and wearable prototypes are shown in this chapter, presenting their fabrication method and functions. We will also talk about the top contributions this dissertation allowed. A third chapter, *Materials, Methods and Results* will firstly introduce the different types of materials used. A second section will introduce the methods and research done with those materials in detail, in order to developed a conductive, stretchable and transferable circuit. A third section shows the results obtained with the different methods and materials applied. Conductivity and strain tests are also performed using different samples, with a final conclusion using a SEM analysis to understand, at a micro-scale, how the material particles interact.

The forth chapter demonstrates the fabrication of multiple prototypes using the fabrication and transfer methods explained in the previous chapter. We produced a capacitive hand-piece for a prosthetic robotic hand, capacitive multi-layer keyboard, headphones with capacitive control bottoms and an EMG tattoo reader. A final chapter will focus on some future works and the publications resulted out of this project.

Chapter 2

State of the Art

The demand for portable and ubiquitous electronic applications generated a great interest in the emerging technology area of conformable electronics: a class of materials and electronic devices that are able to adhere and conform to surfaces. As technology evolves, conformable and stretchable electronics are changing the bio-inspired and bio-integrated technology. In the development of human-device interfaces, their design is primarily focused on portability and comfort to reach a sensation of seamless interaction between the user and the device.

Mostly on-body interface projects aim to create an always-on, unobtrusive, responsive technology that allows the user to interact in a natural and intuitive way with their personal devices and environment, in a direct or passive way.

Since "smaller is better" motto is around the technology world in every project projection and development, a tendency of wearable devices being something more aesthetic and comfortable originated a new term: electronic tattoo (ET) or electronic skin (E-skin). Created to define a variety of devices that can be transferred to the skin, or most common surfaces, and be used to improve the relation between HRI.

The skin is an organ that can sense pressure, temperature and other complex environmental stimuli or conditions. The mimicry of this organ sensory ability using electronics is a topic of innovative research. To imitate tactile sensing via E-skins, pressure sensor arrays are built based on transaction mechanisms and structural designs. Temperature and humidity sensors are also inherent for E-skins. Progress in transmission of data via wireless technology and energy with self-powered E-skins has also been made recently [3], Fig. 2.1.

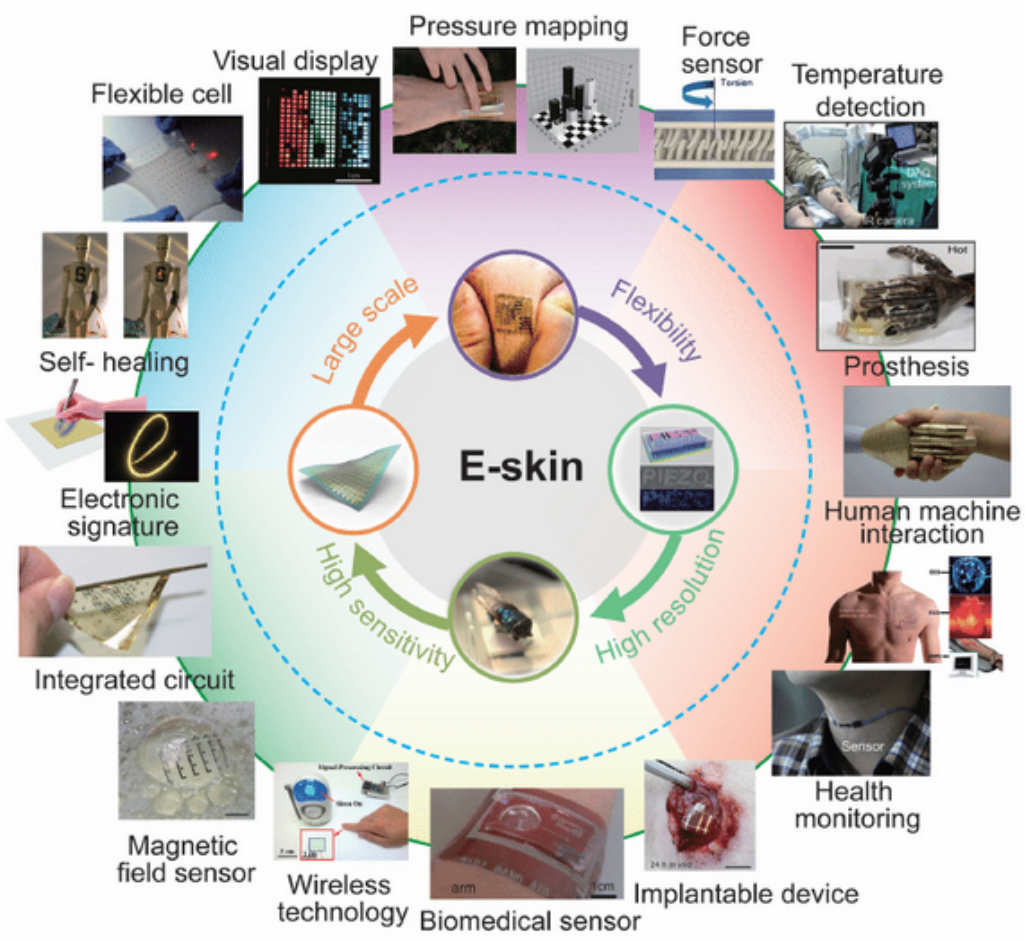

Fig. 2.1 Characteristic properties and diverse functions or applications of recently developed devices for E-skins [3].

Being able to assemble micro-electronic components on temporary tattoo paper substrates or similar ultra-thin transfer polymers, natural and always-available computer interfaces that constantly monitor the output signals can be created [34]. Key applications and innovation driving growth opportunities rely on healthcare, robotics and consumer electronics [35]. Electronic skins are being developed to control electronics, mobile gadgets and enabling next-generation smart devices, also improving healthcare such as vital signs monitoring, healthcare monitoring, prosthetics, wound management, disease/medical diagnostic and drug delivery systems [35].

Bio-monitoring like sweat analysis has been developed by *John A. Rogers et al* [4], into a flexible micro-fluidic device that easily adheres to the skin to measure the user's sweat and show how his or her body is responding to different stimulus, as exercising. Being sweat a rich, chemical broth containing a number of important chemical compounds, this skin interface will change the serpentine channel color, depending on the received health

information by the user's sweat. Integrated wireless connection to a device (e.g. smart-phone) enables to user to record the sweat changes acquired over time.

Fig. 2.2 Sweat-Monitoring device [4].

Producing energy using radio frequency power harvesters electronics is also possible using stretchable E-skin interfaces [36]. This type of results suggest robust capabilities for battery-free future prototypes. Transmitting data from skin electronics to another device is also possible using similar radio frequency, improving the intercommunication between different devices and the user.

Skin temperature sensing tattoos using silicone transfer film and gold (Au) NPs have been recently developed by *Rogers et al* [37]. This type of ET uses Au NPs to form a serpentine wire composed by the heater ($5\mu m$ wide) in one of the extremities, and polyimide layers ($20\mu m$ wide) to encapsulate the Au wire from the environment and reinforce structural support.

The serpentine heater is supplied by an AC current of $3m$A at 0.1Hz frequency. This will change the output voltage depending the skin temperature over time, being able to translate those values to skin temperature values with a dedicated software.

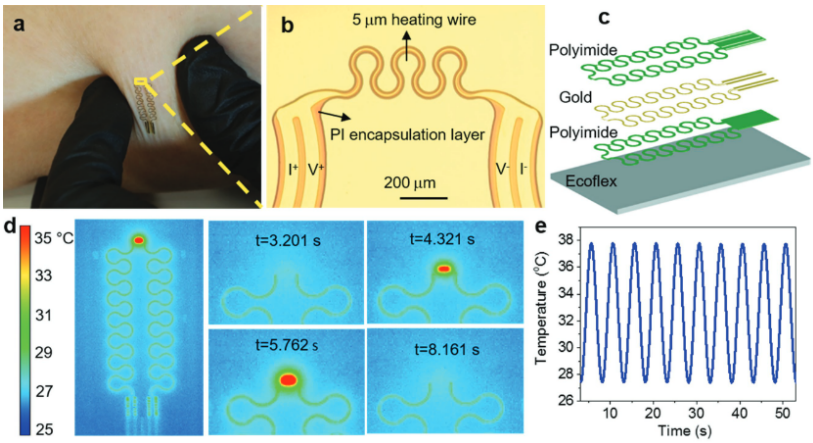

Fig. 2.3 (A) Temperature sensing tattoo, (B) Close-up of temperature sensing tattoo, showing heating wire and Au wires encapsulated with polyimide, (C) Side-schematic of the tattoo, (D) Thermal snapshot of the tattoo on skin, (E) Temperature changing graphic generated over time [37].

Made of "soft" materials that adapt to the mechanical environment properties [38], these use to imitate the mechanical proprieties of the surface when transferred, in this case the human skin. Since they are made with a very low thickness, it allows us to reduce the impact and discomfort of a device previously composed by wires harnesses and buttons. Human skin has natural wrinkles, creases and pits that are in the order of $15\mu m$ to $100\mu m$ [39] and when achieving a smaller thickness in wearable on-skin electronics, the user will not feel the skin unnaturally restrained [40].

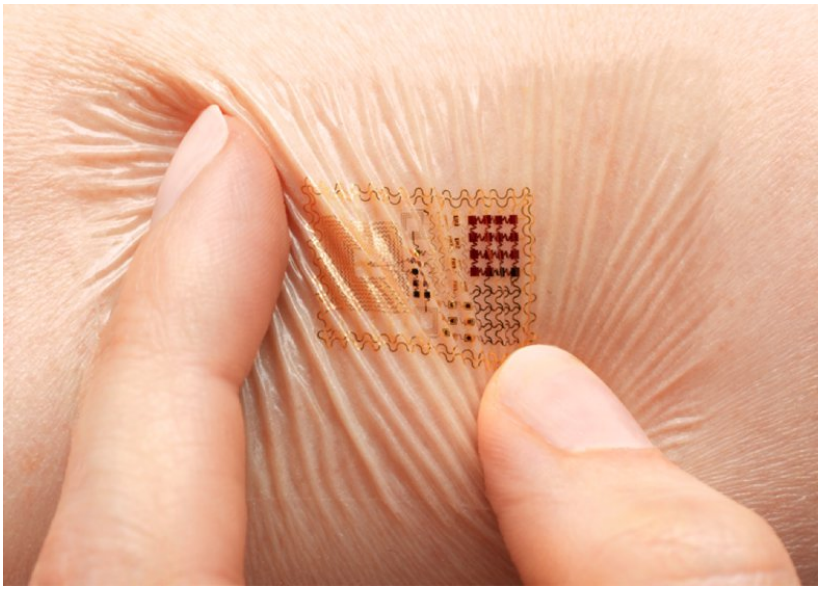

Fig. 2.4 Bio-stamp temporary wireless antenna tattoo.

ET are usually composed by a flexible substrate, may it be silicone, polyvinyl alcohol (PVA), polymeric stamps or skin-safe stickers, which usually don't surpass the $10\mu m$ of thickness. Comfort, safety and bio-compatibility is needed in this type of materials.

They must be safe to use and wear for long periods of time, and since commercially available temporary tattoo paper follows the medical safe usage on human skins, it is desired by most as the optimal substrate [41] [42].

Producing this type of substrates in such an uniformly thin scale requires expensive and complex methods such as a clean rooms, stereo lithography devices, sputtering equipment and expensive materials such as gold sheets [43]. From creating micro-channels filled with LM in a prefabricated substrate or mixing a conductive material such as graphite or silver nano-particles tends to extremely poor conductivity in most of the cases [43].

Our interest rely in develop a method to simplify the fabrication of electronic tattoos. Growing the interest on sinter-free inks, printing directly over the tattoo substrate a conductive path is one of our top objectives to developed different types of applications.

Ink-jet printers are commonly used in households today. Being relatively cheap and commercially available, they became a strong ground to developed methods of printing different types of conductive inks (e.g. AgNP ink and Gallium based LM ink [gallium pdf]), polymers and even solution with living cells [44] [45] over different types of substrates.

The main concept of ink-jet printing is to spray the ink or material in the cartridge on a very specific area of the substrate. Two main types of ink-jet technology are being used to do so, a continuous system or a drop on demand system. It is important to know that water-based inks are ideal for common home printers, since the cartridge nozzles range the size of $8.5\mu m$ to $14\mu m$ [46]. Continuous systems push the ink through the nozzle creating a constant stream. Droplets are deposited on the paper, while unneeded droplets are deflected. This type of technology has the advantage of operating at higher speed than drop on demand systems.

Drop on demand (DOD) systems spray the ink through the nozzle when a drop is desired on the page. DOD can be divided in two types, continuous ink-jet and phase change ink-jet [44]. In the first case, the droplet path is controlled by the reaction of two charged plates. Due to the constant flow, the cartridge nozzles are less likely to become clogged or dry. Continuous DOD ink-jet uses thermal or piezoelectric cartridges to release the ink from the cartridges.

While thermal print-heads use current to heat a nozzle section and spray the ink into the substrate, piezoelectric print-heads use pressure to force the ink to be sprayed, Fig. 2.5.

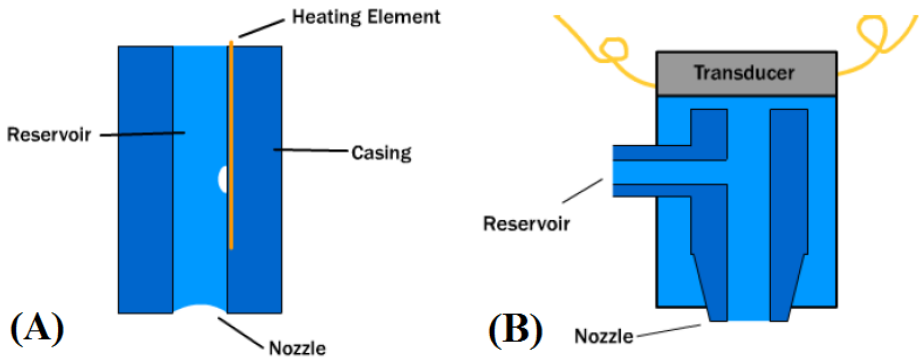

Fig. 2.5 (A) Thermal print-head, (B) Piezoelectric print-head.

A phase change ink-jet includes a phase change of the material to be printed. Usually filled with a waxy solid material, the print-head melts it using heat and spray the now liquid material into the substrate using continuous jet technology. The material then returns to the waxy solid state. This type of material has the advantage of being able to bond directly with some types of substrates without the need to be absorbed.

Conductive inks are now being reported and used in ink-jet printers for flexible electronics. Commonly used silver/gold nano particles (NPs) are being used to draw conductive paths in different types of polymers for 3D MEMs devices [47]. This type of materials are dispersed, via sonication processes, in solvents (e.g. alcohol). After printing, they require sintering processes at high temperatures (>100ºC) to remove the remaining solvents in the substrate.

Gallium-based liquid metal (GBLM) inks being in a liquid state at room temperature do not require sintering processes like the previous materials. Not being based on colloidal NPs, GBLM inks do not have clogging issues, however, they behave like a gel rather than a true liquid for being readily oxidized in air contact [48]. Specialized sinter-free inks, as the silver nano-particle Mitsubishi ink available commercially for regular ink-jet printers [5], are made to use directly on ink-jet printer's cartridges, although, a specific media is needed to make the ink conductive [5].

After printing, the silver nano ink particles accumulate on the surface of the special media selectively *(1)*, and the chemical sintering agents diffuse, from the micro-porous layer *(2)*. Dispersing agents react with the chemical sintering agents and come off from the nano particles *(3)*. The AgNP then fuse together and transform into a silver foil *(4)* as we see in Fig. 2.6.

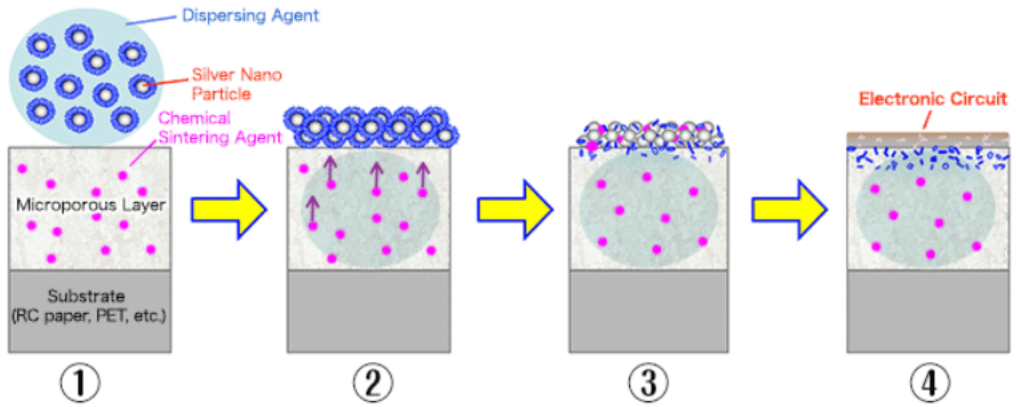

Fig. 2.6 How AgNP Ink obtains conductivity [5].

Even solving this problem, commercially available conductive inks are not flexible or stretchable after drying, which poses a problem since electronic tattoos need to adapt to the skin or the surface changing dynamics. To overcome this, researchers apply different techniques such as laser cutting black graphite to define the conductive path and also the pattern of the tattoo itself, turning the electrical layer into an aesthetically customizable layer, but never using directly the transfer substrate only [43].

Other options, like stencil lithography, are used to pattern the conductive circuits, at the cost of losing the easy customizable and printing patterns. Within this work, a method was discovered and allows turning a non-conductive AgNP ink over a substrate into a conductive and stretchable ink that can be used over TTP and transferred to any surface.

2.1 Contributions

Based on the shortcoming of the current materials and methods of fabrication of printed electronics, and with the goal of achieving electronic tattoos and hydrographically-transferable 3D conformable electronics, this work provides contributions over the state of the art materials and fabrication methods in several domains.

- Propose material combinations and methods that allowed to functionalize currently available silver nano-particle (AgNP) inks alloyed with liquid-phase eutectic gallium-indium (EGaIn) metal, which increase the conductivity of silver ink in an order of magnitude of 6, not requiring complex and labour intensive processes, as high temperature sintering or clean rooms.

- This allows printing conductive AgNP ink over temporary transfer paper (TTP), being able to develop desired circuits and transfer them to a wide range of surfaces, materials and three dimensional shapes.
- In addition, the proposed process shows results in a stretchable ink alloyed with LM that keeps conductive even after 60% of total size stretch. This is an useful and important feature for applications of in-mould electronics, where vacuum moulding is used to transfer circuits to the parts.

Chapter 3

Materials, Methods and Results

In this chapter we describe the materials and methods used during the realization of this dissertation. This includes the initial commercial conductive ink, secondary alloys used for conductivity increase mechanisms, substrates used to transfer the circuits to body and 3D parts, and a printer which was used in the printing of these circuits, and how it was modified to accommodate the requirements of the project.

Due to the vast diversity of materials available, either conductive or non-conductive that can be used to produce these types of conductive circuits in a specific substrate, it is impossible to work with all the products commercially accessible. However, some background knowledge and tests were made in order to choose from an extensive list, the ones with the best potential to work combined with others.

3.1 Materials

3.1.1 Substrates

The first priority was to find a suitable substrate that could sustain five major tests due to our final ambitions in this project.

- **Flexible** - Since a main objective is apply and transfer to the many types of surfaces the printed circuits, and develop wearable applications and devices with flexibility and stretchability.
- **Comfortable** - The material used in the substrate needs to be, ideally, less than $100\mu m$ to fit within the natural user's wrinkles, to feel natural and skin conforming.
- **Resistant** - Remain fully operational for hours or days without the need of any maintenance or fixes. Being water-proof and heat resistant is needed too.

- **Porous and Absorbent** - Since the ink is being printed above the substrate, a porous and absorbent material is needed for the ink to remain fixed after dried. A hydrophobic substrate will not work for example.
- **Aesthetically Customizable** - Being able to take any shape for any printed size is desired for future aesthetic purposes in different types of projects.

Following this 5 conditions, we chose to use an inkjet-printable temporary tattoo paper for our purposes (Silhouette Inkjet Printable Tattoo Paper) [49]. This type of paper is composed by a thin flexible plastic film, bonded to a back protective layer with an intermediate material which is soluble in water. When the paper comes in contact with the water, the protective back layer starts absorbing the water until the in-between material starts to dissolve, releasing the two pieces from each other Fig. 3.1 (A). After adhering to the desired surface, it is water resistant and can sustain temperatures up to 180ºC.

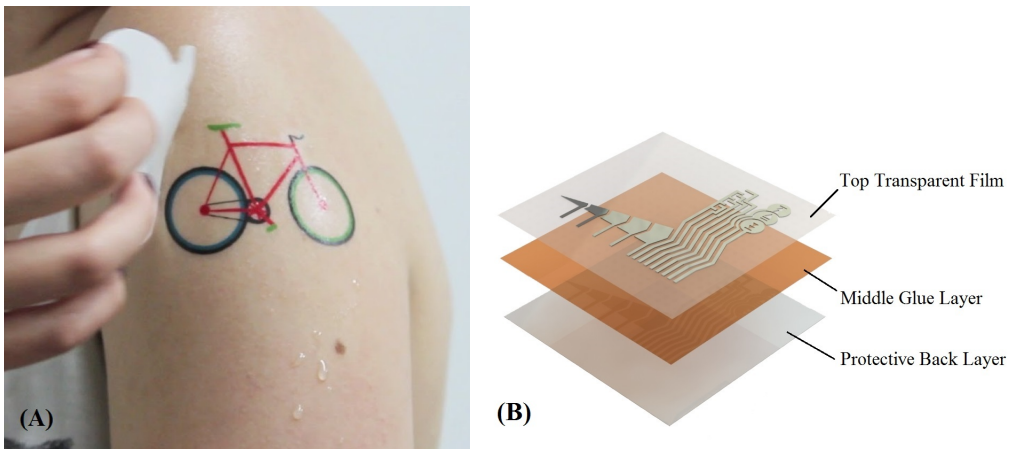

Fig. 3.1 (A) TTP layers being separated (white paper removed refers to the protective back layer, transparent film with the drawn pattern to the transferable film), (B) Side Schematic.

A second type of substrate used is composed by polyvinyl acetate (PVAc), which is commonly referred to as wood glue, white glue or school glue, and is a synthetic resin prepared by the polymerization of vinyl acetate [50]. This type of substrate is printable, and when in contact with water an emulsion occurs, creating a type of glue that after drying, can remain unaltered from -70ºC to 281ºC. This type of temperature range is useful to resist heat sintering processes and material wear [51].

PVAc is commonly used in the industry nowadays to print graphic designs into three-dimensional objects. Mostly used as adhesive for porous surfaces, this type of substrate and process is seen on all types of products used everyday (e.g. flash-lights, automotive pieces).

PVAc can be transferred to almost any type of material, including metal, plastic, wood and fabrics, using water-transfer methods, Fig. 3.2.

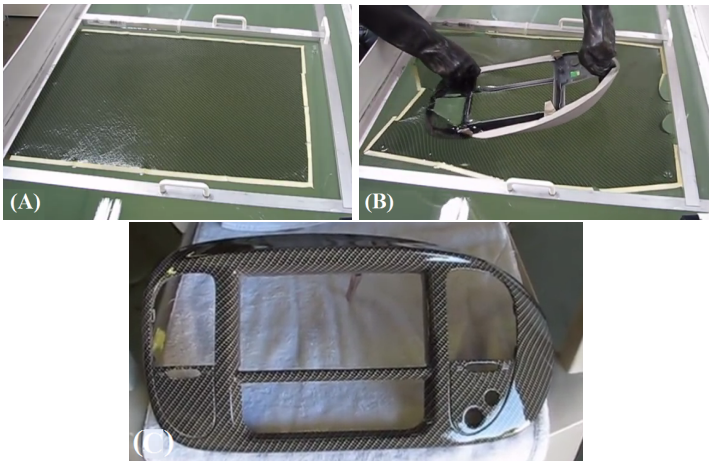

Fig. 3.2 (A) PVAc with printed design is placed on the surface of a container filled with water, (B) After the PVAc emulsion has finished when reacting with water, the pattern can be transferred to the desired surface, in this case, a automotive piece, (C) The final result after drying for a few hours at room temperature.

3.1.2 Printer and Cartridges

Since directly printing a circuit over the substrate is needed, an ink-jet printer will be used after certain modifications. Although the TTP is flexible like a regular office paper, it is thicker and harder to bend and to avoid unnecessary waste of TTP due to hard creases, we decided to modify a HP840C printer, Fig. 3.3, to print in a single direction without the need to bend and twist the paper like regular common printers do nowadays.

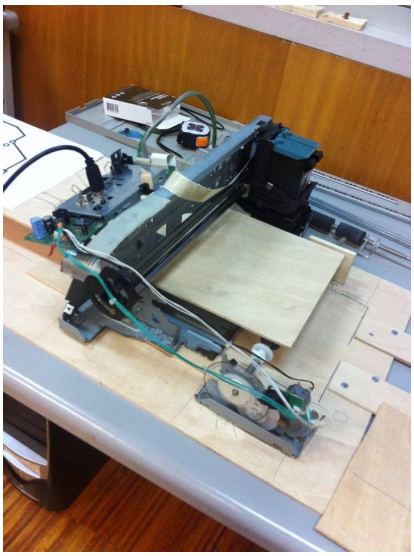

Fig. 3.3 Modified HP840C Printer

This printer uses Drop-on-demand thermal ink-jet printing, with a resolution of 600 x 600 dpi. To modify this printer, first, we remove the protecting cover and disassemble the important printing components to later re-assemble them. A printer commonly has a feeding motor to make the paper move while printing, controlled by a laser sensor encoder. The paper is fed via feed rollers, Fig. 3.4.

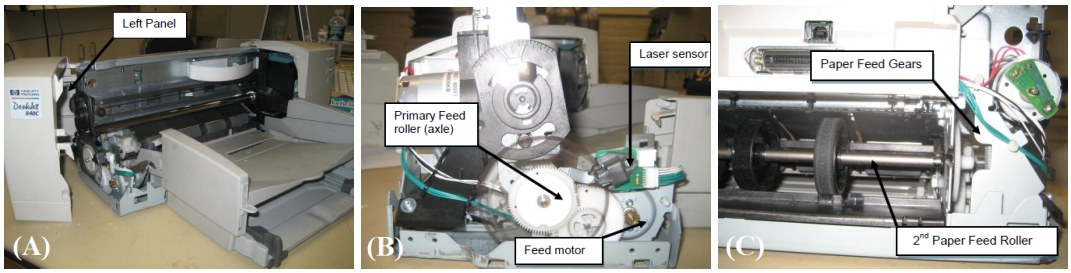

Fig. 3.4 (A) Removing the outside case, (B) Side view, showing the laser encoder and paper feed motor, (C) Rear view, showing the paper feed gears and the second paper feed roller, now removed.

Reassembling the main components was done to allow us to adjust the height of the printer, which can be useful for different types of substrates in the long-term, like thicker and not-flexible substrates especially (e.g. PCB boards, hard plastic surfaces). The ink cartridges used for this printer are the C6615 series cartridges, with a 15mL capacity [44], Fig. 3.5. This type of cartridge is enticing to use for being easy to clean and refill with the conductive ink.

Fig. 3.5 C6615 Series cartridge without side cover and open.

To clean and refill the cartridge, a hole is drilled with 2.5*mm* diameter. The clean process is made by pouring, through the drilled hole, warm water and removing it, repeating the process until no ink is found inside. When the cartridge is fully clean, the conductive ink is poured into the cartridge's hole using a syringe, and then sealed with hot-glue. It is now ready to be placed onto the printer's head.

3.1.3 Inks

Many types of nano-particle inks and powders are available nowadays (e.g. gold NPs ink, cooper NPs ink and power, manganese nano-powder, silver nano-particles and nano-powder). For this project, we will be using a conductive silver nano-particle ink (*NBSIJ-MU01*), from Mitsubishi Paper Mills Limited [5], having an universal use for home ink-jet printers. With a very low resistance after dried of 0.1Ω it is an ideal choice.

Having a density (1.200 g/mL), viscosity (2.30 mPa.s) and surface tension (32.0 mN/m) very similar to regular ink-jet inks, clogging issues will not be a problem. Since most copper and gold NPs inks require special printers and printing nozzles, using them in regular home printers would mostly clog the cartridge nozzles, since they are based on colloidal NPs [48].

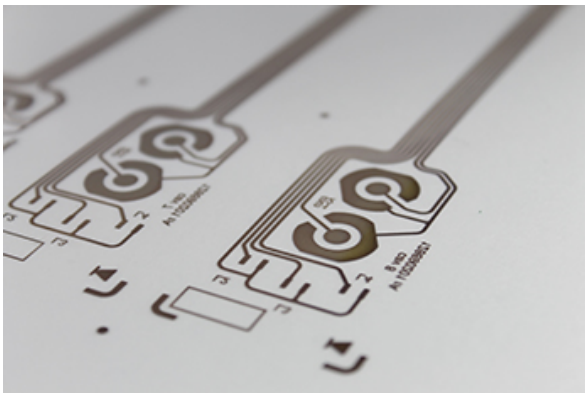

Fig. 3.6 Silver Nano-Particle ink printed circuit.

Mitsubishi silver NP ink has an advantage of drying at room temperature after an hour, while most of other inks require high temperature sintering processes, higher than 100ºC [48]. This ink having the ability to dry at room temperature requires a special media to have good conductivity. The media absorbs the undesirable solvents composing the ink (e.g. ethanol) leaving only the conductive silver traces on the surface [5]. If no special media is used, the ink will have a not so desirable resistivity (>20MΩ).

3.1.4 Conductive Silver Polymer Paste

This product (reference *C2080415P2*) is a thermoplastic screen printing ink developed by SunChemical. Being flexible, one will use this conductive silver polymer paste (CSPP) to fix micro-electronics and wires in the substrate and printed circuits.

The paste remains in a viscous state at room temperature, turning into a hard rubber material after heat sintering processes. To sinter the CSPP, a heat gun is used for 5 to 10 minutes at 130ºC to 170ºC. Alternatively, baking at 130ºC to 150ºC for 10 to 15 minutes will have the same effect. Epoxy conductive silver paste, not requiring sintering processes, is a potential fixing material that will be tested in future works.

3.1.5 Liquid Metal

We discovered that a Gallium-Indium liquid metal alloy can increase the conductivity of the silver ink. At room temperature, LM is able to alloy with the printed AgNP ink. For this reason, we choose LM for its ability to act jointly with the AgNP printed traces when the substrate is stretched and un-stretched. This is proven later in this dissertation. If only AgNP ink is used when the substrate is stretched or bended, it tends to break the printed traces and form cracks and thus become non-conductive.

The most commonly used liquid metal is Eutectic Gallium Indium (EGaIn), which is a Gallium-based alloy. Gallium and Indium are not as toxic as similar materials (e.g. mercury (Hg)) and are generally safe to interact with [52]. Gallium is a trace nutrient, while Indium has been used before as dental filling.

Fabrication of LM just consists in weight the right material proportion of 75.5% Gallium and 24.5% of Indium and mix them in a hot place at 195ºC for 24 hours. This will melt both materials to a liquid state and bind them together, remaining in the liquid state at room temperature after.

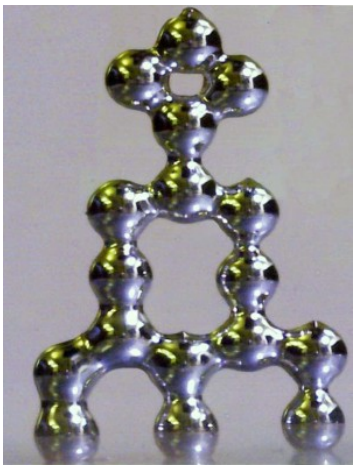

Fig. 3.7 Liquid Metal deposition due to oxide layer.

Furthermore, EGaIn has electrical properties similar to rigid metals, at the cost of being more expensive than other materials (e.g. gold nano-particles). Rapid advances were made on fabrication methods of EGaIn based electronic [53], including stencil lithography [54], laser patterning [55], micro contact printing [56] and additive manufacturing [57].

Recently, an effort on direct ink-jet printing of liquid metal was made in [58], where authors could successfully jet EGaIn nano particles over a substrate. Yet, due to the semi-conductive oxide layer around the LM Nano particles, with a thickness of 0.3 to 1 nanometre [59], the deposited traces are not conductive immediately after deposition. This requires more labour processes to turn the printed traces conductive, consisting usually on applying pressure over them or using other types of chemicals to remove the oxide layer temporarily (e.g. HCL vapour).

3.1.6 Acetic Acid Solution and HCL Vapour

When alloying LM with silver ink printed circuits, excessive LM will be all over the substrate. To remove this excess, an anti-oxide agent is needed to remove the oxide layer

around liquid metal particles. Doing so, the metal loses its bonding with the substrate and resembles into the minimum surface energy structure (a spherical ball).

Acidic solutions remove this type of oxide layer around the liquid metal, and recently done with a ionic solution (e.g. salt water) and a battery. Acetic Acid or NaOh solutions (e.g. kitchen vinegar), with a percentage of 5-7% can be used to remove this oxide layer with little effort in a controlled concentration. More aggressive substances of corrosive character like HCL acid or vapour are used to remove the oxide layer more easily, but possibly damaging the substrate and the traces if the concentration is not well balanced.

For this reason, selecting the appropriate method to remove the oxide layer depends on the substrate material and the bonding between the silver ink and the substrate. Using an Acetic Acid Solution (AAS) prepared with kitchen vinegar (7% acetic acid concentration) will be used to remove the oxide layer. To prepare this solution, a container is filled with $\frac{1}{5}$ of vinegar, and the remaining portion with regular tap water. Increasing the percentage of vinegar will make the solution more aggressive against the oxide layer.

Pure HCL with a 37 *wt%* concentration will be used to created vapour inside its own container. With a syringe, one can collect the vapour inside and use it in cleaning methods explained in the next section. While working with HCL acid, protection is necessary to avoid injuries.

3.2 Methods

In this section, we will talk about fabrication methods to create a conductive, transferable circuit. Using mainly temporary tattoo paper (TTP), other substrates are used to prove the method works. Using the modified printer, AgNP Mitsubishi ink is used in this process to print the desired circuits.

Fabrication of conductive AgNP circuits include four main steps:

- **(A)** - Ink-jet printing the circuits using AgNP ink;
- **(B)** - Deposit and spread LM over the printed circuit and substrate to alloy it;
- **(C)** - Clean the excessive LM from the substrate;
- **(D)** - Transfer the working and clean circuit to the desired surface.

Depending on what to develop, the surface of the circuit and the way one wants it (exposed or not), will change the way to proceed in some of those steps.

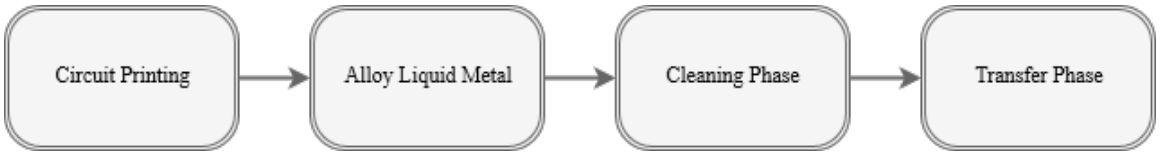

Fig. 3.8 Phases required to make a conductive circuit with Ag and LM.

The first step, *(A)*, is to ink-jet print the desired circuit created with the previously chosen AgNP ink.

To design the circuits, *Eagle Software* is used. This software is commonly used to design PCBs' multi-layer circuits with the advantage of being free. Circuits designed will have a maximum size of an A4 sheet (210 x 297 millimetres). This limit is due the modified printer only being able to print with a maximum width of 210*mm*.

After printing the circuit, a drying stage takes place. It can take up to one hour to fully dry at room temperature (25ºC), or using a heat-gun to accelerate the process.

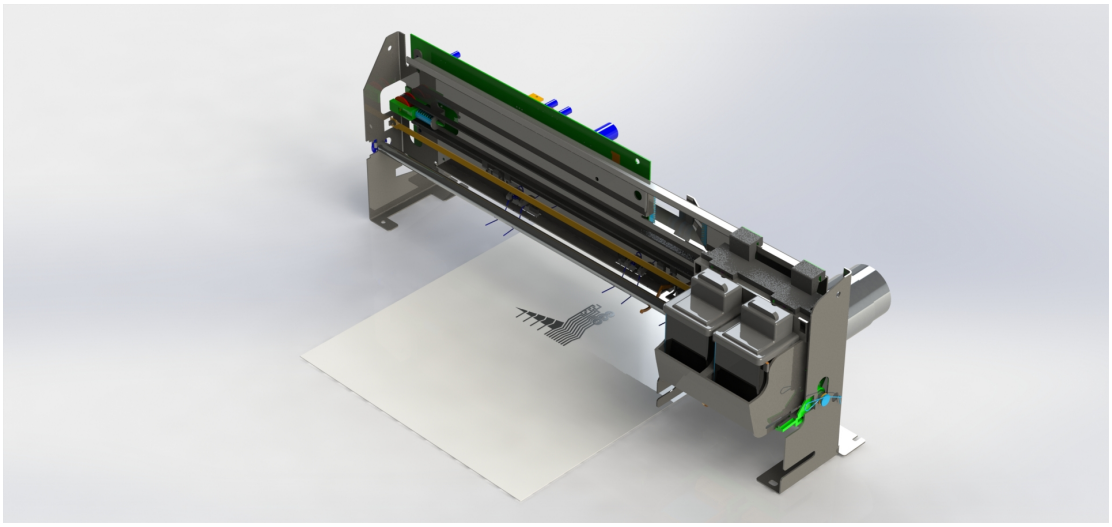

Fig. 3.9 Printing a circuit with AgNP Ink.

In this process's second stage, *(B)*, LM is alloyed to the AgNP printed circuit, now dried. Using E-Gallium-Indium LM, we apply with the help of a syringe small portion of it over the substrate, Fig. 3.10 (A).

Using a soft brush, roller or soft fabric, the deposited LM is then spread and gently rubbed over all the substrate. Exploring this method, we concluded that soft fabric works better at this stage. This mainly happens considering that the mechanical controlled pressure by the user triggers the bonding between the LM and the underlying surface better, Fig. 3.10 (B).

No stencil is used at this stage and LM is spread all over the substrate surface. The printed circuit is hidden below the LM layer along with the substrate and whole area is conductive, Fig. 3.10 (C).

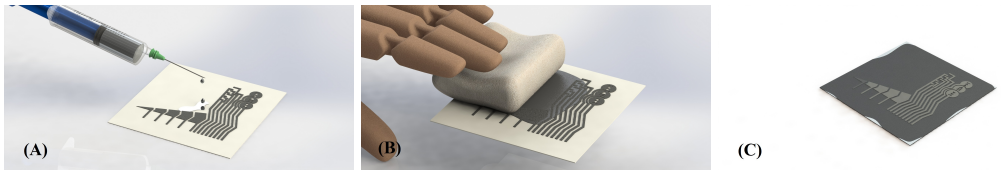

Fig. 3.10 (A) Deposition of LM over the substrate, (B) Spreading the LM, (C) LM spread over all the substrate.

The third step, *(C)*, consists in cleaning the excessive LM over the substrate, but still leaving it alloyed to the silver printed circuit. To do so, two different methods are used. An acetic acid solution (AAS) or hydrochloric acid (HCL) vapour.

Using an AAS, the acidity should be high enough to remove the LM from the substrate without being too aggressive to rupture the bonds between the printed circuit and the LM particles. A 7% AAS mixed with $\frac{4}{5}$ of water in bottle is found to be enough for this purpose. The solution is then poured over the substrate, specially the area to be cleaned and leave to rest for 10 to 15 seconds. When the solution gets in contact with LM, the metal loses its bonding with the substrate and resembles into the minimum surface energy structure (a spherical ball). Yet, it remains in the traces since the bond is stronger, Fig. 3.11 (A). The TTP is then tilted to one side, removing the solution and the excessive LM from the substrate. This process can be repeated until the substrate is fully clean, leaving the silver circuit traces now alloyed with LM.

The printed circuit which was hidden below the LM appears again, but it is significantly shinier due to the chemical reaction between the silver ink, the LM and the AAS, in addition to the conductivity of the traces being increased substantially, Fig. 3.11 (B).

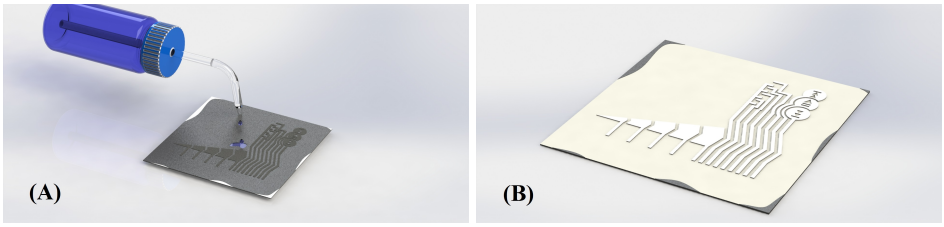

Fig. 3.11 (A) Applying the acidic solution, (B) Cleaned substrate.

Other alternative to clean the substrate is using HCL acid vapour. With the help of a syringe, the vapour is sprayed over the substrate. This method also worked equally, but

required much more control, since the vapour can be too aggressive if sprayed too close, or have a null effect if sprayed too far from the substrate. This can be an optimal method for high scale and autonomous production of circuits, in consideration of not being as invasive as an AAS on the substrate. The first method is safer and easier to handle in the lab environment overall.

The fourth and final stage, *(D)*, of the process is transfer the clean and conductive AgNP traced alloyed with LM to the desired surface. Prior to transfer we are able to fix micro-electronic components (e.g. LEDs, micro-controllers, wires) to the traces and substrate with a conductive silver polymer paste (CSPP).

Assembling the micro-electronic components requires an intensive labour process. The components are placed in the desired area, Fig. 3.12, to be fixed or connected to other conductive paths and components. Due to their size, the use of a microscope is sometimes required.

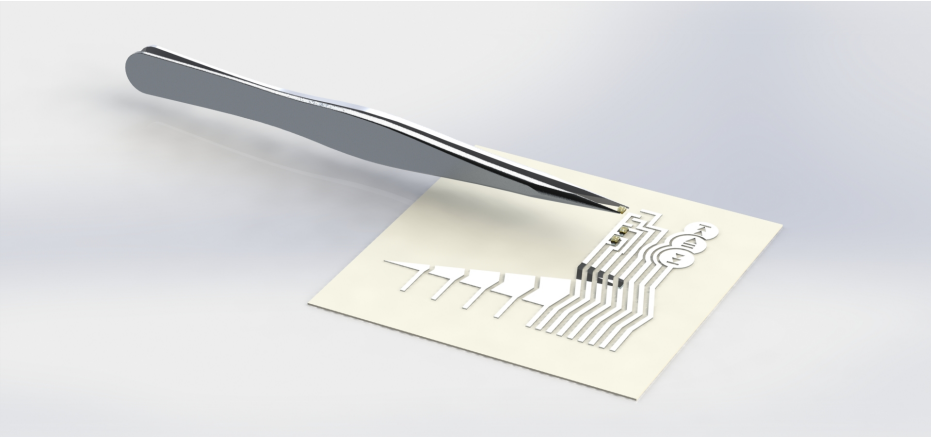

Fig. 3.12 Placing a small LED on the circuit using a pincer.

Using a syringe, the CSPP is then used to connect the component in the fixing area or conductive pads using a small drop, Fig. 3.13. A final sintering process is required to cure the silver paste, using a heat-gun at 130ºC for 5 to 10 minutes, lowering the paste resistivity to 45$m\Omega$/sq.

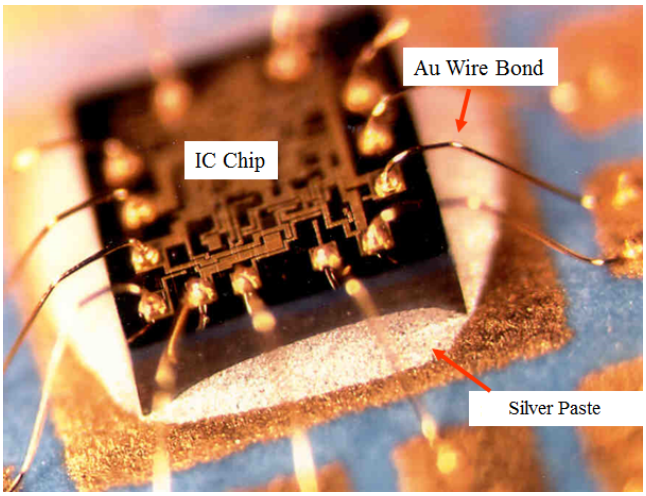

Fig. 3.13 IC Chip fixed in a PCB using silver paste.

Posterior to assembling all the micro-electronic components, the circuit can be transferred to the surface using hydro-graphic transfer (also referred to as water-transfer printing or immersion printing). This method, as explained previously, is used when exposing the circuit is needed.

Usually, the use of water-transfer methods have advantages when leaving the circuit exposed. One has ground for adjustments such as micro-electronic re-assembling, and most importantly, insulation from the surfaced transferred. The TTP film is not conductive, hence the printed circuit having no contact with the surface where it is transferred on. The steps for water-based transfer method are presented in Fig. 3.14.

Although, a direct transfer method can still be used if we want a direct contact between the transfer surface and the printed circuit and components. In this case, the printed circuit will directly face the surface. It is commonly used when EMG technology is applied.

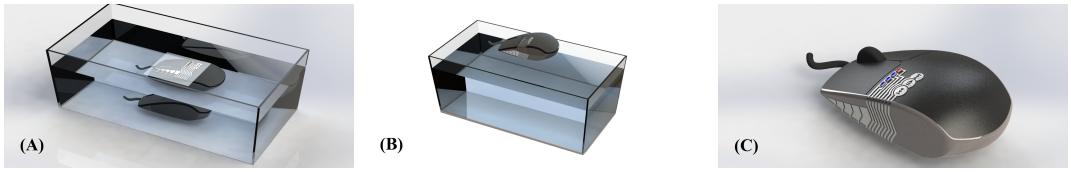

Fig. 3.14 (A) Immersed 3D printed Mouse Piece with TTP film floating above, (B) 3D printed Mouse Piece grabbing the TTP film into its surface, (C) Final result.

In Fig. 3.14 (A), while still on its carrier film, the circuit is placed on top of a container filled with water. The host surface is immersed inside, in this case a computer mouse shell, to have the circuit transferred. Previously cleaning the host surface from grease and dirt is

recommended, and can help avoid small surface air bubbles that get fixed to the surface when submerging it.

After a few seconds, the protective back layer of the temporary tattoo paper separates from the top layer. A reaction between the water and the PVAc mid layer detach both parts. A real example is shown at Fig. 3.15 where a 3D printed piece is being used as the host transfer surface with the TTP film floating in the water. This piece will be used in a robotic hand, explained in other section.

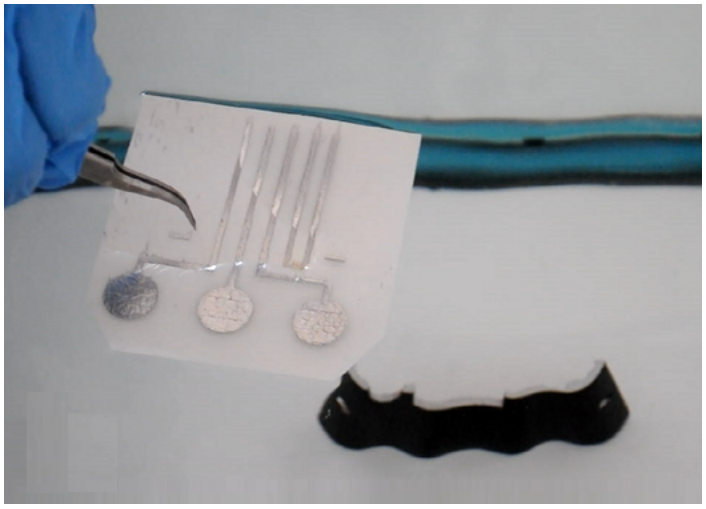

Fig. 3.15 Host surface submerged in the water container and floating TTP above.

The host surface is then raised from the bottom of the water filled container, Fig. 3.14 (B), attaching with the floating conductive TTP transfer film. In this phase, adjusting the host surface position with the TTP film is crucial. This process gives us a lot of manoeuvrability to fit the TTP film to any shaped surface. It conforms to porous and curved shapes smoothly.

An important advantage when using TTP transfer film is the ability to bend 180º degrees on itself or a surface, preserving the same conductive proprieties. This is very useful in multi-layer circuits and for interfacing with other rigid electronics, removing the need to use regular wires. Since the TTP thickness is very small ($10\mu m$), we can avoid unnecessary holes, coverings and protections in the surface or object, Fig. 3.16.

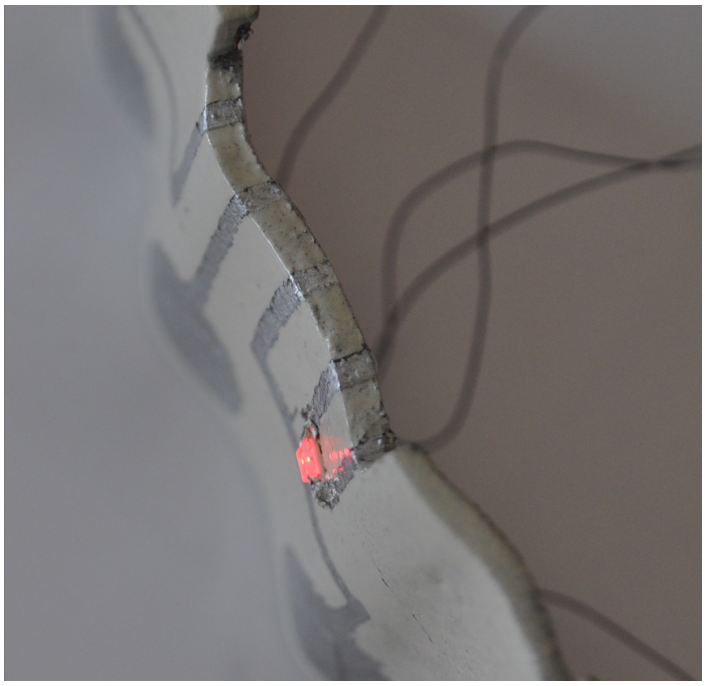

Fig. 3.16 3D Printed piece with a conductive TTP circuit curving around the surface.

Posterior to removing the host surface from water with the attached TTP film a drying step is needed. Since TTP is a temporary substrate, the attachment strength with the surface will degrade over time. For this reason, a protective cover using transparent plastic paint or a similar material (e.g. PDMS) must be done. To complete this step, drying the surface and the transferred film is done using an heat-gun for 2 to 5 minutes. The protective layer is then applied, sealing the surface and the transferred film. This way, it can sustain wear, temperature changes, humidity and water.

When a direct transfer method is used, all the process repeated equally but the last stage. The circuit is directly applied on the host surface, with the printed circuit facing it and still with the protective back layer, illustrated in Fig. 3.17 (A).

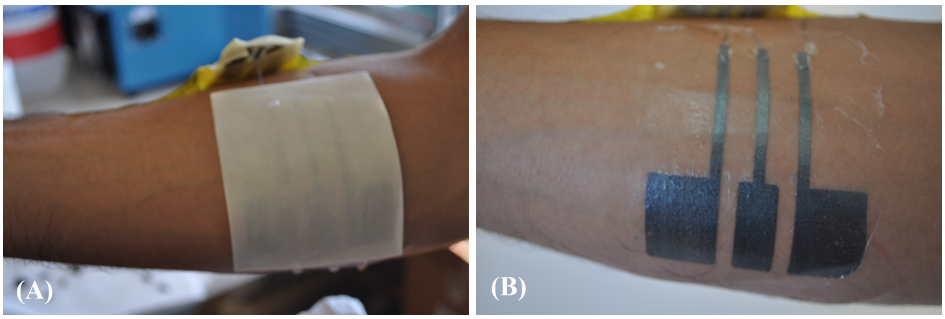

Fig. 3.17 (A) Tattoo Transfer Paper applied directly on the skin with protective back layer, (B) Tattoo Transfer Paper fixed on the skin with protective back layer removed.

On top of the protective back layer, water and pressure are applied. Doing this, the water is absorbed by the protective back layer and the bond between the tattoo film and the protective layer is broken, due the reaction with water and the PVAc mid layer. Released the back protective layer, only the TTP film remains in the surface, Fig. 3.17 (B).

Other Materials

In order to prove that LM alloys with AgNP ink is, initial tests were performed over two additional substrates, PVAc and Tracing Paper (TP).

A hydro-graphics PVAc film was tested. Interest on this substrate has grown for being used to transfer decorative graphics over shaped surfaces parts that are exposed to harsh environments, requiring resistance against high and low temperatures, water and humidity and general wear (e.g. car wheels). Hydro-graphics PVAc transfer film contains a water soluble polyvinyl acetate (PVAc) layer that in a semi-liquid state adheres to the surface, adapting to its shape and becoming a hard plastic after dried.

This type of substrate is composed by two main layers, a bottom layer made of a removable protective paper and top layer composed of PVAc, with a hydrophobic coating, Fig. 3.18.

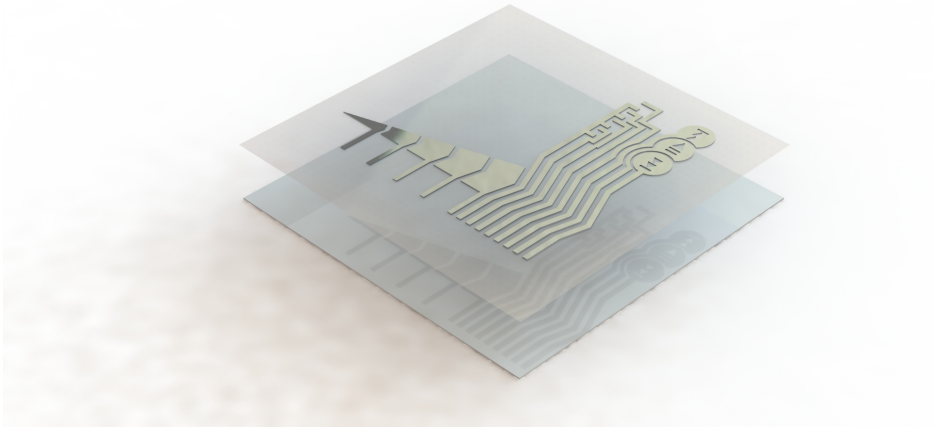

Fig. 3.18 Polyvinyl acetate composing layers.

To test this substrate, a circuit was printed with AgNP ink in the PVAc top layer. After the drying process of one hour at room temperature (25ºC), a layer of LM is applied over this layer, including the printed circuit, using soft fabric or a roller.

The cleaning process is done using HCL vapour only. Since PVAc's top layer is not as hydrophilic as the TTP film, using an acetic acid solution (AAS) would cause the AgNP ink

to wash away. This happens considering the ink is not absorbed enough into the PVAc's top layer when printed.

Using the right concentrations, flow intensity and distance when applying the HCL vapour, the substrate is cleaned from the excessive LM and leaving the AgNP traces bonded with the LM only. Mostly due to the vapour concentration not being strong enough to break the bond between the silver particles and the LM, but being able to remove LM from the substrate. Using 1M HCl solution mixed with ethanol showed to have the best results.

Increasing the vapour flow intensity or concentration will break that bond and even sometimes damage the substrate due to HCL's corrosive character. Reducing them will neither remove the excessive LM from the substrate nor the traces.

Unlike TTP, PVAc substrate can only be transferred using water-transfer methods. We start by removing the back protective layer by hand, 3.19 (A). The PVAc film with the printed circuit is now placed on the water floating, similar to TTP. A reaction between the PVAc and the water will turn the PVAc film into a viscous, semi-liquid state. While this reaction happen, wrinkles can form in the film, but after a few seconds, they tend to disappear, 3.19 (B). Note that this type of substrate is only possible to be transferred from above, making the conductive circuit and components always face the surface where it is going to be transferred 3.19 (C). When trying to transfer from bellow using an immersed host surface, the PVAc will break apart due to the water surface tension, making the circuit traces not conductive any more.

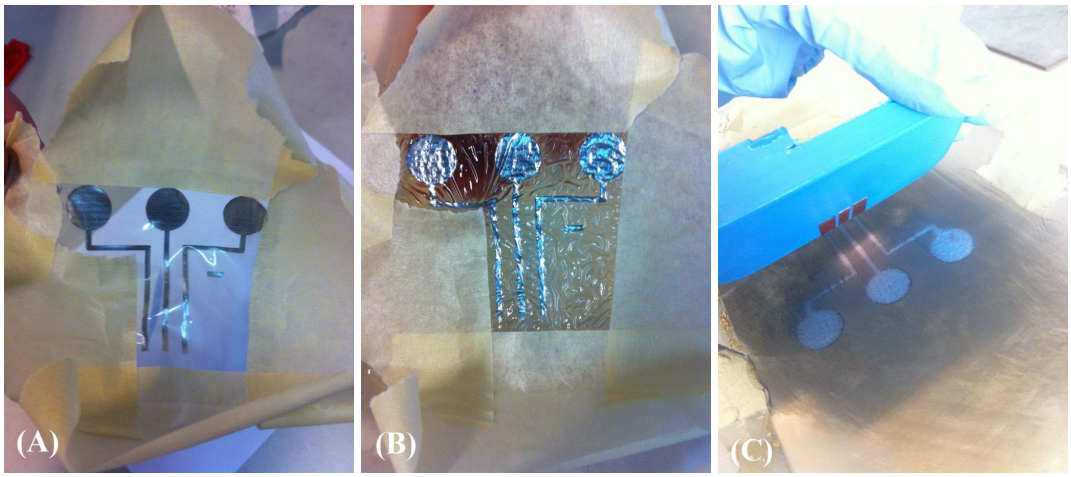

Fig. 3.19 (A) Removing PVAc protective back layer by hand, (B) PVAc forming wrinkles due to the reaction with water, (C) Transferring the PVAc circuit to the host surface, from above.

Following to transfer the PVAc substrate along with the conductive circuit to a host surface, a drying process is necessary. It takes one hour at room temperature (25ºC) to fully

dry, becoming a rigid plastic material and bonding strongly to the object and sealing the circuit. The sealing PVAc's characteristic turns the material very durable and resistant to harsh environments and wear.

A third substrate that was tested was tracing paper (TP), Fig. 3.20. Since tracing paper is porous, the ink is quickly absorbed and dries faster than the previous substrates. Contrary to previous substrates, tracing paper is not meant for transferring and is only used to demonstrate and confirm that AgNP ink binds with LM particles. Since it is a natural hydrophilic substrate, when an acetic acid solution is used the paper will fully absorb it and damage the printed pattern. For this reason, using HCL vapour, similarly to PVAc substrate, results in good and conductive final results.

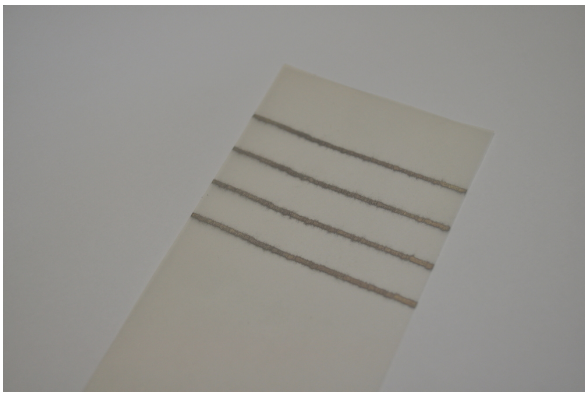

Fig. 3.20 Tracing Paper with conductive lines.

3.3 Results

Some tests will be performed to gather precise information regarding the printed conductive traces and circuits. The measurement of the conductive trace's resistance is going to be analysed, prior and posterior to alloy and clean, with a batch of ten samples. The same samples will be stress-tested using a stretching machine that record the resistance while stretching to a defined distance. A scanning electron microscopy (SEM) is used to analyse the different element types behaviour with others, and to understand how the particle connection works.

3.3.1 Conductivity

Conductivity is the degree to which a specified material conducts electricity, calculated as the ratio of the current density in the material to the electric field which causes the flow of current. A low resistivity indicates a material that readily allows the flow of electric current.

Table 3.1 Average resistance change for lines of $40mm \times 1.5mm$ over different substrates and with different cleaning methods.

	TTP	PVAc	Tracing Paper
Silver-Ink only	20,24 MΩ	not conductive	not conductive
LM + Acetic Acid Mixture	10,25 Ω	NA Ω	NA Ω
LM + HCL Vapour Cleaning	12,91 Ω	56,18 Ω	182,61 Ω

A multimeter is used to measure the resistance on three different substrates (TTP, PVAc and Tracing Paper) with printed lines, before and after the EGaIn deposition.

To test the line resistance, we print ten lines with $40mm$ length and $1.5mm$ width. The conductivity is tested first with AgNP ink only. After alloying the printed lines with LM and cleaning the excessive LM with an AAC solution, the same measurements are performed again. TTP substrate, after the LM deposition and cleaning, has the conductivity increased by almost two million times. Initially, the printed circuit with AgNP ink only has a resistance average of 20.24MΩ. Cleaning with an AAS increases conduciveness and thus reducing the average resistance to 10.25Ω. The HCL vapour works in a similar way, reducing the line's resistance to an average of 12.91Ω, as Table 3.1 shows.

This corresponds to a sheet resistance of $5.06M\Omega/sq$ before alloying LM and $2.6\Omega/sq$ after alloying LM and cleaning with an AAS. The sheet resistance is calculated on thin films that have an uniform thickness. It is invariable under scaling of the film contact and therefore can be used to compare the electrical properties of devices that are significantly different in size. It is done using $R = \rho\frac{L}{A}$, where R is measured resistance, ρ the sheet resistance ($\Omega.cm$), L the length, and A the cross-section area. This cross-section area is calculated using the sheet thickness, t ($10\mu m$), times the width, W ($1.5mm$).

On PVAc and Tracing Paper substrates, the initial AgNP ink printed circuit is non-conductive. On both substrates, applying an acetic acid solution to clean the substrate will damage the circuit and remove the AgNP ink and LM. This occur due to the absorbing and porous surface characteristics. For that reason, HCL vapour will be used to clean the substrates to obtain conductivity after the process is completed.

PVAc substrate has an average of 56.18Ω when cleaning and testing ten samples with the same line length and width previously tested ($40mm \times 10mm$). With the tracing paper, resistance average is 182.61Ω, as Table 3.1 shows. This resistance difference is justified by the two substrates opposing characteristics, yet proving that a link between AgNP ink and LM is formed in the alloying process.

The 180º Turn

Temporary tattoo paper has a sharp feature found: the 180º bend. TTP can turn on itself while keeping the printed circuit traces conductive, keeping the traces resistance unchanged. This feature makes it possible to pass conductive traces through very small fissures with the size of the paper thickness (around $10\mu m$). While being a simple advantage, this is extremely useful to make the use of wires and channels obsolete, while saving space and keeping a good aesthetics.

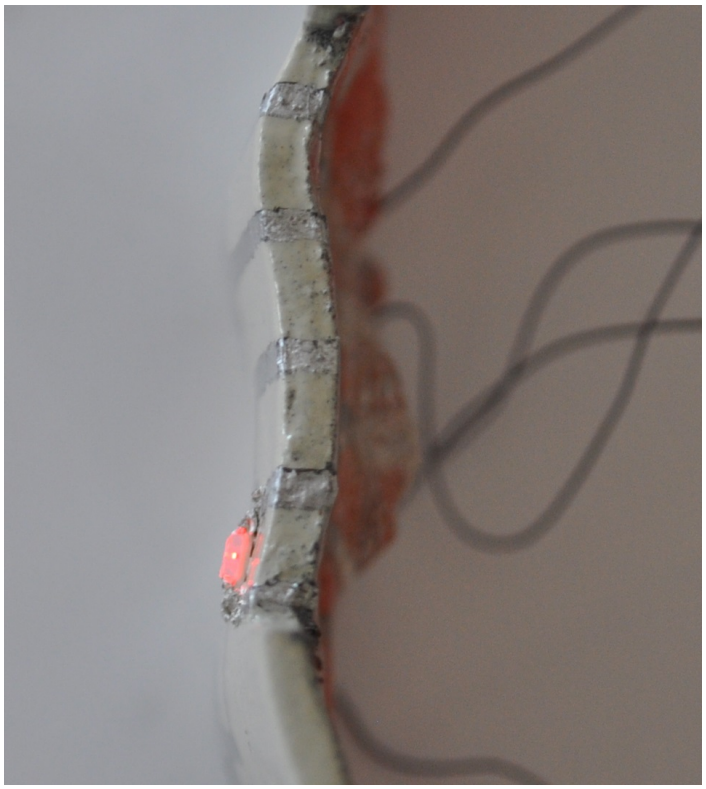

Fig. 3.21 180º Turn close up in a 3D printed piece, using TTP

This technique is also possible using PVAc, but slightly harder due to the semi-liquid state the material is when transferring it to the host surface.

3.3.2 Strain Tests

Performing uni-axial tension tests provide an effective and easy way to characterize a material's response to different loads. To perform uni-axial tests, the sample displacement is held at a constant rate, while reporting the displacement and the changing resistance of the sample.

Ten conductive samples with 60*mm* length and 15*mm* width lines were printed on TTP substrate with AgNP ink, alloyed with LM and cleaned afterwards. The samples were transferred to a bottom cured PDMS layer with 1*mm* thickness. To measure the resistance, two conductive wires were attached to each end of the lines and fixed using CSPP. Another PDMS layer is placed above and cured, with a final result shown in Fig. 3.22.

Fig. 3.22 Some of the samples used in the strain tests.

This method described as "sandwich method", Fig. 3.23, is commonly used to encapsulate micro-channels and stencil-lithography with LM in PDMS.

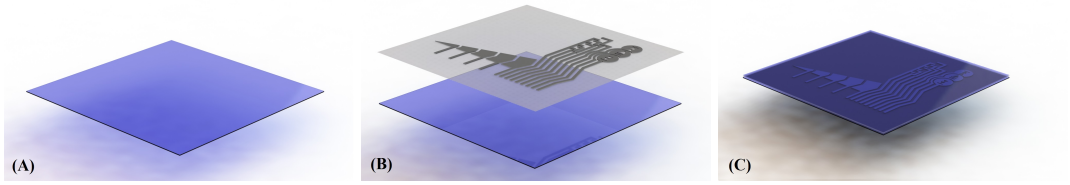

Fig. 3.23 Sandwich method explained. (A) Bottom cured PDMS layer, (B) TTP film transferred to the bottom PDMS layer, (C) Encapsulating top PDMS layer.

A stretching device is developed using an *Arduino Mega 2560* Board and a stepper motor. The board can control the stretching speed, distance to stretch and repetitions designated by the user, Fig. 3.24. This board will also send real time information to an interface console via a COM port connected between the Arduino Board and the computer. Time, repetition number, distance travelled and line resistance is listed each 500 milliseconds. Using this data, resistance changes over time can be analysed.

The sample is then fixed to the device's grabbing points. Guided by the definitions set by the user, the device will stretch the sample until it reaches the set distance and returning to the initial position. This is repeated for the number of repetitions the user sets. Each one of ten samples will pass a twenty repetition cycle, stretching for 40*mm* from the initial position and record the resistance changes over the process.

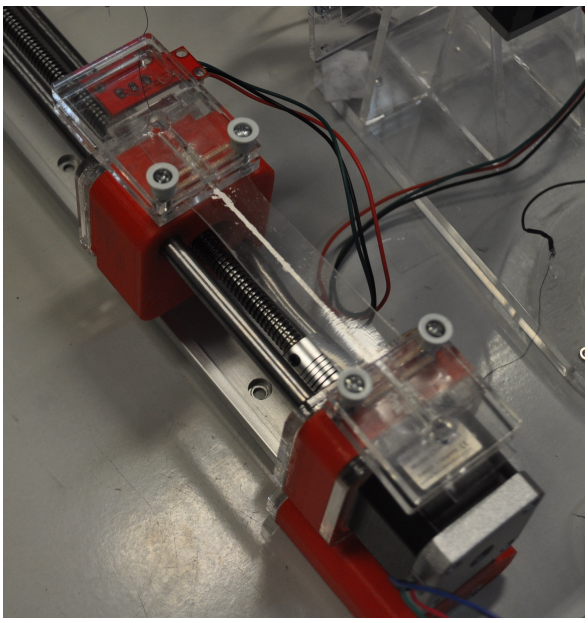

Fig. 3.24 Device used to stretch the line samples.

The results with TTP encapsulated with PDMS reveal a very good stretchability for both materials. The lines remain conductive in the several times the material is stretched and unstretched. Although, the resistance increases on each repetition. Starting with an average resistance of 36.4Ω, each cycle increases the resistance measured until it stabilizes at 181.2Ω after twenty cycles. Fig. 3.25 shows the result when testing one of the samples.

Some down peaks were observed during the stretching tests. These events mainly happen due to the LM characteristics such as surface tension. When the line is stretched, LM will lose the bond and a material refit takes place. A new conductive path is formed with higher resistance, but in some cases when unstretching the line, a better and less resistive path is found.

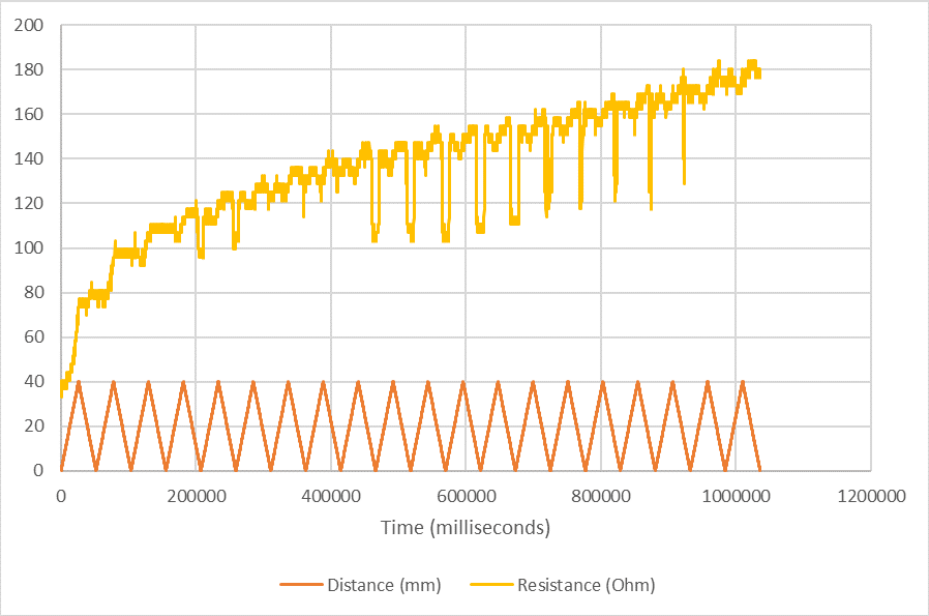

Fig. 3.25 Result of one sample test. Orange trace represents the average resistance and the red trace the distance travelled (40*mm*) from the original position on each repetition cycle.

Breakpoint stress tests were also performed to obtain the maximum length the samples can be stretched. A huge stretching distance was defined (100*mm*) to make sure the material would fail, breaking the sample or losing the conductivity. Testing ten samples, nine out of ten would break apart when the critical distance was reached. The remaining sample just lost the conductivity without breaking. Critical distance is located between a 45*mm* to 55*mm* stretching interval, corresponding to 75% to 91.6% of strain. The average strain achieved before the samples break was 85.1% with a standard deviation of 4.9%. Before the sample breaks, the resistance reach peak values. A sample test is shown in Fig. 3.26 with orange dots representing the breakpoints for the remaining samples.

After 20 cycles the sample is still conductive. Nevertheless, the resistance is increasing after each cycle, meaning that some of the connections between Ag-eGaIn clusters are destroyed. However, on some of the samples one can see a sharp decrease of the resistance when stretch is released. This suggests that some of the connections between the clusters are restored after releasing the stretch.

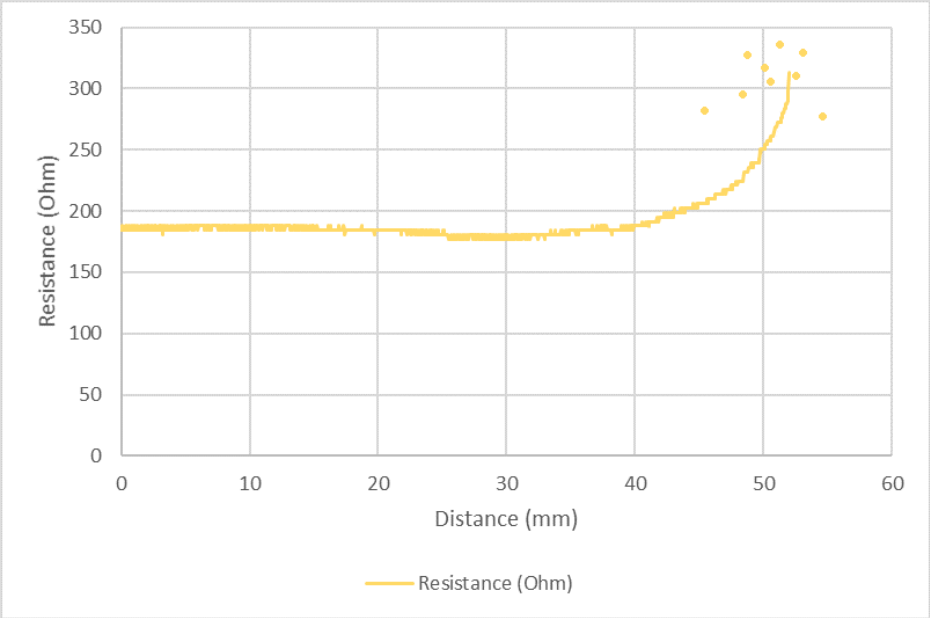

Fig. 3.26 Breakpoint test results for one sample tested (continuous orange line) and orange dots representing the breakpoints for the remaining samples.

Samples break due to the method applied to encapsulate the TTP (two layer "sandwich") and air bubbles trapped inside the material, resulting in weaker points. The resistance is stabilized around 180Ω prior to test since a twenty repetition test was performed before with the same samples.

3.3.3 SEM Microscopy

To understand how different materials bind and react with each other, a Scanning Electron Microscopy was performed, also knows as SEM. This type of electron microscope produces images of a sample by scanning the surface with a focused beam of electrons. As electrons interact with atoms on the surface, different types of signals that contain information about the sample's surface topography and composition are produced [60].

Samples used are composed of printed AgNP ink, before and after the EGaIn alloying and cleaning process, on a TTP substrate. This section is divided in two main parts, one to observe the samples by increasing the magnification from 10x to 10kx, using the backscattered electrons mode (BSE or BSD). A backscatter electron mode detects elastically scattered electrons, which have a higher energy from atoms below the sample surface. Using a BSE allows the use of lower vacuum levels, reducing sample preparation requirements and minimizing beam damage.

Before alloying the LM to the AgNP printed ink circuit, as Fig. 3.27 (A) shows, many cracks on the surface are observed. This is the main reason a printed circuit with silver ink only is not very conductive. Increasing the magnification to 100x, 1kx and 10kx (Fig. 3.27 (C), Fig. 3.27 (E), Fig. 3.27 (G)) we observe the cracks formed by the ink solvents and composts at a higher magnification.

Fig. 3.27 (B) displays the reaction between LM to the AgNP after the alloying and cleaning processes. Major cracks can still be found, while the smaller ones were filled by the LM deposition, increasing the conductivity and reducing the trace resistance by thousands. Fig. 3.27 (H), with a 10kx magnification, shows the interaction between LM and silver particles.

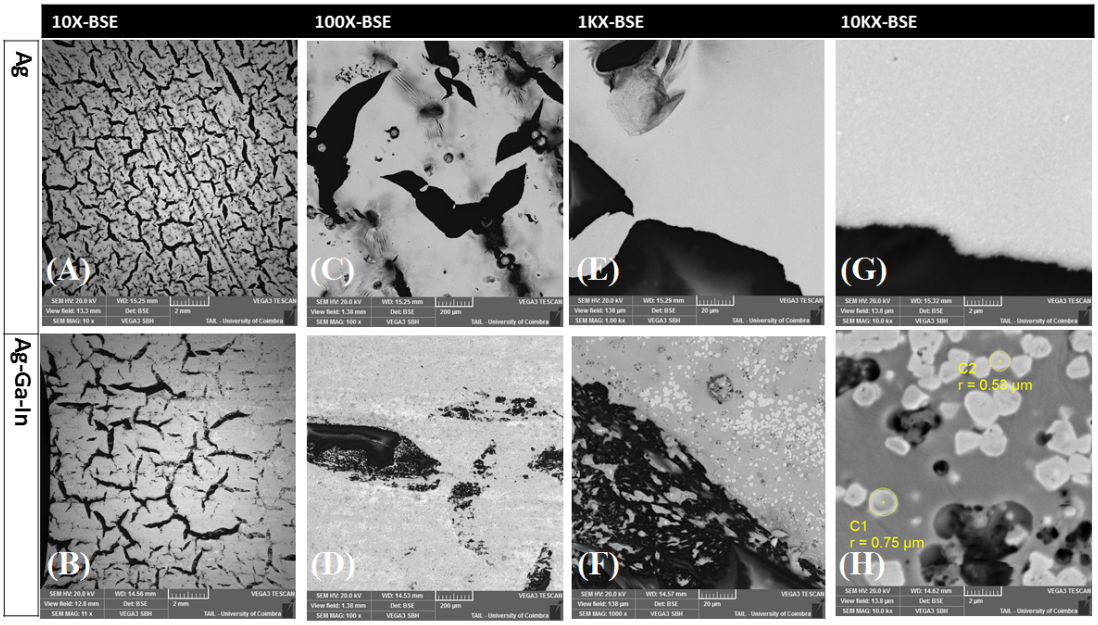

Fig. 3.27 (A,C,E,G) AgNP printed trace on TTP before alloying LM at different magnifications, (B,D,F,H) Final result after alloying and cleaning the AgNP printed trace with LM at different magnifications with AAS.

Images from AgNP printed samples show an excellent distribution of silver nano particles over the substrate. Ag-GaIn samples, however, show the creation of particle clusters as well as silver-free spaces. The clusters sized around $0.5\mu m$ are observable in Fig. 3.27 (H) with a 10kx magnification. This suggest that the Gallium-Indium induces particle aggregation, which helps confirming the increasing electrical conductance by a better percolating network. This analyse proves that the LM alloys with the AgNP ink on most of its printed trace. Since Mitsubishi Ink only has a 15% of pure silver, a purer ink with more silver percentage could

result in a better alloying and initial conductivity, reducing the risk of unalloyed zones that can cause the trace non-conductive.

SEM Microscopy - Elemental Analysis through Energy-Dispersive X-Ray Spectroscopy

In this type of analysis, the different chemical elements are analysed at different layers. Similar to the previous SEM microscopy, tests will be performed on samples printed with AgNP ink only, and samples with printed AgNP alloyed with EGaIn.

The first sample to be analysed is printed with AgNP ink only. A elemental map of carbon (C) in red, and silver (Ag) in blue is represented in Fig. 3.28 (B). The carbon element is present due to the TTP protective back layer which is composed primarily by regular absorptive paper. Silver, as expected, is shown due to the ink used to print the trace.

Scanning the elemental percentage on the blue zone composed essentially by silver, displays a high percentage of silver as expected (96.17%), followed by oxygen (O) with 2.11% and carbon (C) with 1.71%, as Fig. 3.28 presents. The same scan performed in the red zone reveals a percentage of 75.67% carbon and 20.43% oxygen, expected in regular paper. Tiny percentages of other elements are found due to the paper composition, Fig. 3.28 (D). This means that TTP mid layer, composed by PVAc, may have some other elements that help in the release process between the protective back layer and the TTP top film where the circuits are printed.

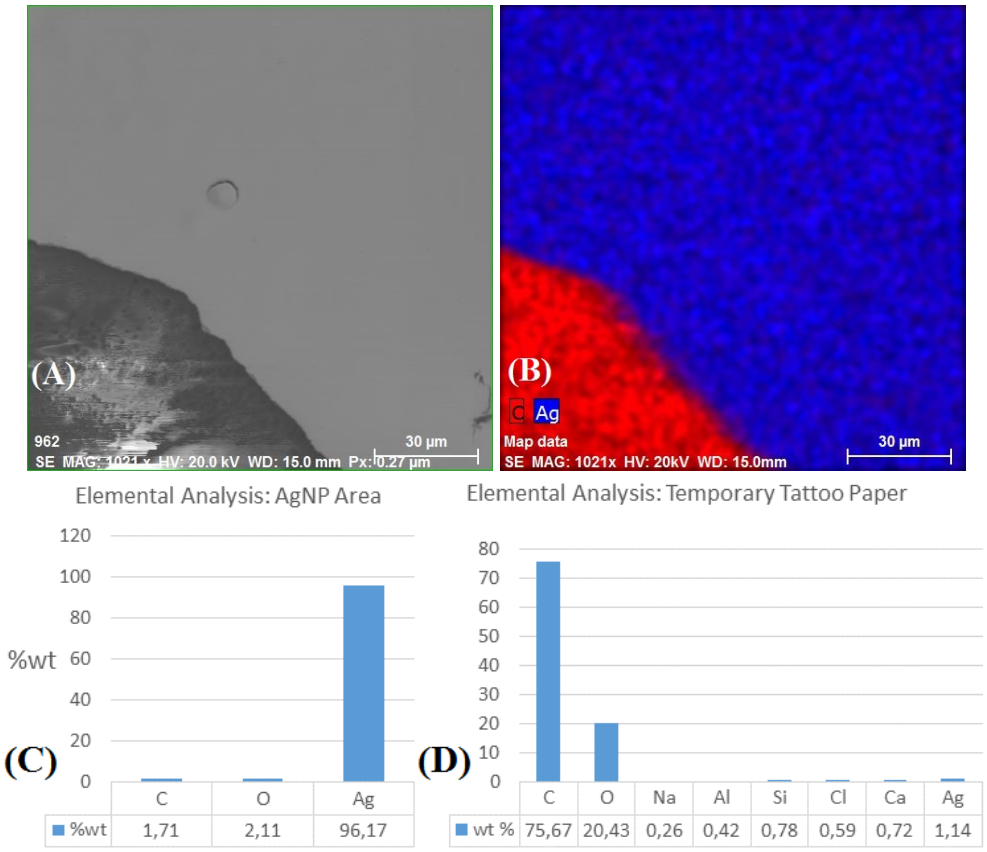

Fig. 3.28 (A) BSE scan on the sample surface showing the frontier between AgNP printed ink and the substrate, TTP, (B) Elemental Analysis through Energy-Dispersive X-Ray Spectroscopy, showing in red the substrate and in blue the Ag element, (C) Percentage of each element in the scan performed

Repeating the same analysis with a Ag-GaIn sample reveal major differences compared to the Ag only samples. Two main zones are found performing an elemental scan: grey zones and bright zones, Fig. 3.29 (A). When analysing and comparing Fig. 3.29 (A) and Fig. 3.29 (B), one can assume the bright zones have more silver concentrations. Grey zones on the other hand have no silver detected.

A percentage composition analysis is performed to have a precise percentage of one of each composing elements in both zones. Bright zones have a silver percentage of 43.85%, 18.39% of gallium and 26.4% of indium, Fig. 3.29 (F). In grey zones, silver is non-existent, while gallium composes 57.1% and indium 20.24%, Fig. 3.29 (E). Due to this, one can say silver clusters are formed in bright zones when alloying and cleaning processes are performed. Silver particles move to form clusters during these processes, losing the initial silver uniform distribution.

The ratio of indium to gallium is 26 to 74 in grey zones, Fig. 3.29 (E), which is very near to the original alloyed EGaIn percentage (24.5-75.5). In grey zones, more carbon is also found compared to bright zones (19% vs 4%), suggesting Ag-GaIn does a better coverage of the substrate where bright zones exist.

Finally, the ratio of Indium-Gallium in the bright zones is 59 to 41, Fig. 3.29 (F), (from the original 24.5-74.5 EGaIn concentration), suggesting that Indium has a more important role in the formation of these clusters. This also explains the resistance of the circuit to smearing or marking, since there is a phase shift from the original liquid EGaIn to a solid Ag-GaIn material. In addition, the new composition suggests that during the cleaning process some of the gallium should have been removed from the substrate.

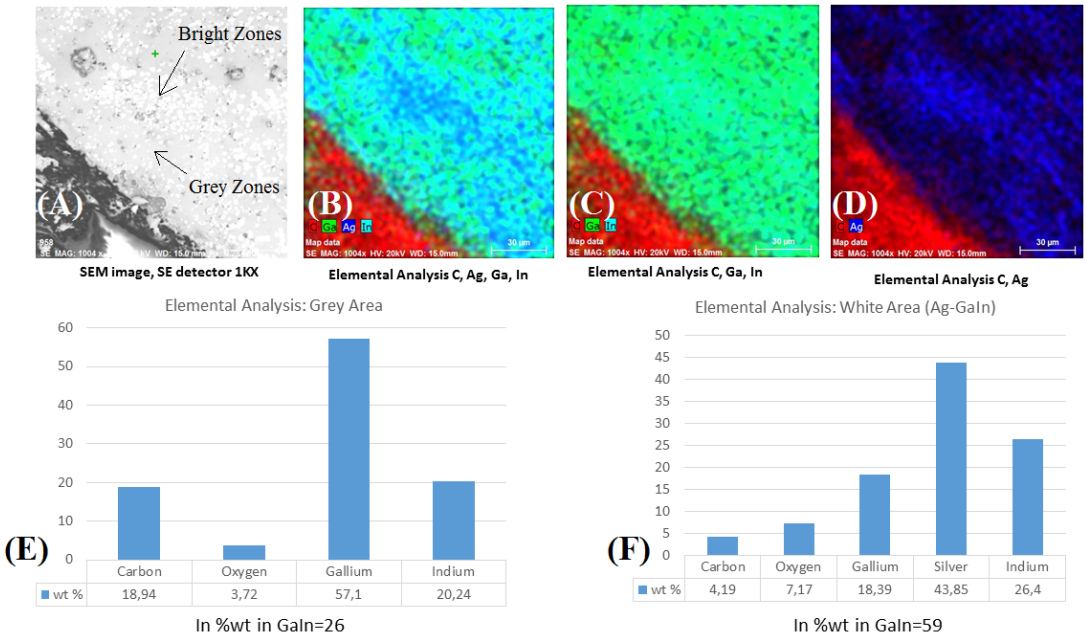

Fig. 3.29 (A) SEM Microscopy performed reveals bright and grey zones at 1kx magnitude, (B),(C),(D) Elemental analysis with different types of elements selected, (E) Elemental percentage analysis for grey zones, (F) Elemental percentage analysis for bright zones.

Even though extensive analysis were made to understand how the different elements react in the presence of others through the different process stages, more expensive and time-consuming methods can be performed in the future to improve our understanding in this matter.

3.4 Conclusion

A new method was developed for printing and transferring conductive circuits over various surfaces. We addressed several challenges in this field and discovered a new patent pending material composition and process which can be used in various applications.

The material composition and the overall process was presented, showing that this process can turn non-conductive samples into conductive. Conductivity increase of over a million times was reported over three substrates, e.g. temporary tattoo paper, PVAc water-transfer paper and tracing paper.

Additional tests proved that the used ink is also stretchable which is an important factor for several novel applications, such as vacuum forming and transfer of printed electronics into various three dimensional surfaces.

Finally, with a detailed SEM analysis the precise composition of the conductive traces were carefully investigated, showing the exact mechanism in which the conductivity increase happens.

Chapter 4

Case Studies

In order to show that hydrographic electronic circuits are a technology that fits in nowadays demands, in the research and consumer field, they must hold some crucial characteristics. Improving interaction between the user and device while keeping the good aesthetics is a main objective. This type of technology can be applied not only in the healthcare field but also in nowadays simple gadgets.

In this section, five main case studies are studied:

- A 3D printed hand piece is created with three capacitive bottoms to allow the user to change the prosthetic hand's fingers synergy.
- A capacitive multi-layer keyboard developed using temporary tattoo paper and PDMS. This keyboard is flexible and stretchable and used to improve underwater works, high temperature environments or to use as a gadget.
- A headphone with integrated capacitive bottoms in the outside cover. This will allow the user to manipulate volume, change sound tracks and turn the device "on" or "off" with a simple finger touch.
- An EMG reader tattoo is used to acquire muscle movements depending the hand position and movements.

4.0.1 Capacitive 3D Printed Hand Piece

Previously, a robotic prosthetic hand was developed to grasp various objects with different hand synergies. The fingers' tips are produced with capacitive sensors that will detect the shape of the object, applying a specific movement to close the hand until a threshold is reached and avoid damaging the object, yet grasping it. In this prototype, the user has no

input and can not control anything, since the process is fully automatized. Our goal is to adjoin three capacitive bottoms to allow the user to have more control over the robotic hand (e.g. fully close the hand when pressing a bottom). A red LED will be included to blink when one of the bottoms is pressed. To start with, a 3D printed piece is made and will be used as host surface for the conductive circuit. This piece will fit in the prosthetic robotic hand, Fig. 4.1.

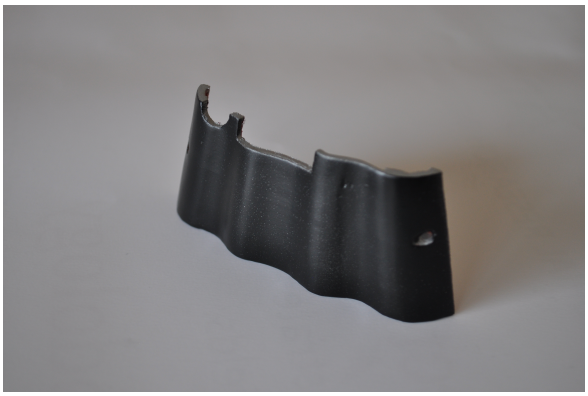

Fig. 4.1 3D printed piece to fit in a robotic prosthetic hand.

The three bottom and LED circuit schematic is printed over TTP substrate using AgNP ink, Fig. 4.2.

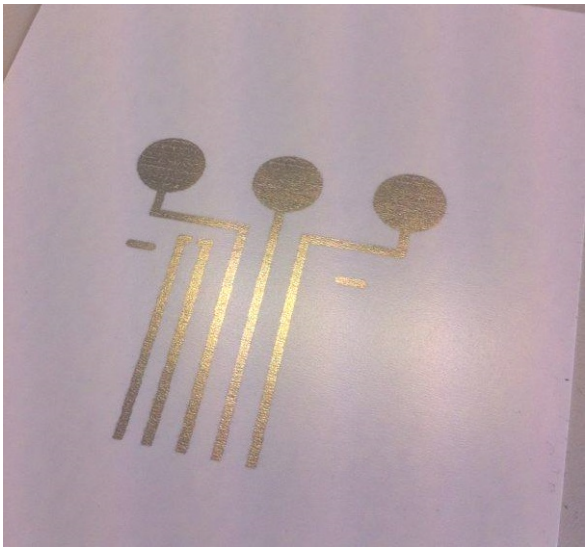

Fig. 4.2 Printed circuit schematic on TTP.

After the circuit dries for one hour at room temperature (25ºC), we will now place and alloy LM over the circuit and substrate. Using a syringe filled with EGaIn LM, we place

little drops over the substrate, Fig. 4.3 (A). With the help of a soft paper, mechanical pressure is applied using our hand. This will help in the alloying process between silver and LM, Fig. 4.3 (B). After this stage is completed, the final result is an evenly distributed LM over all the substrate, Fig. 4.3 (C).

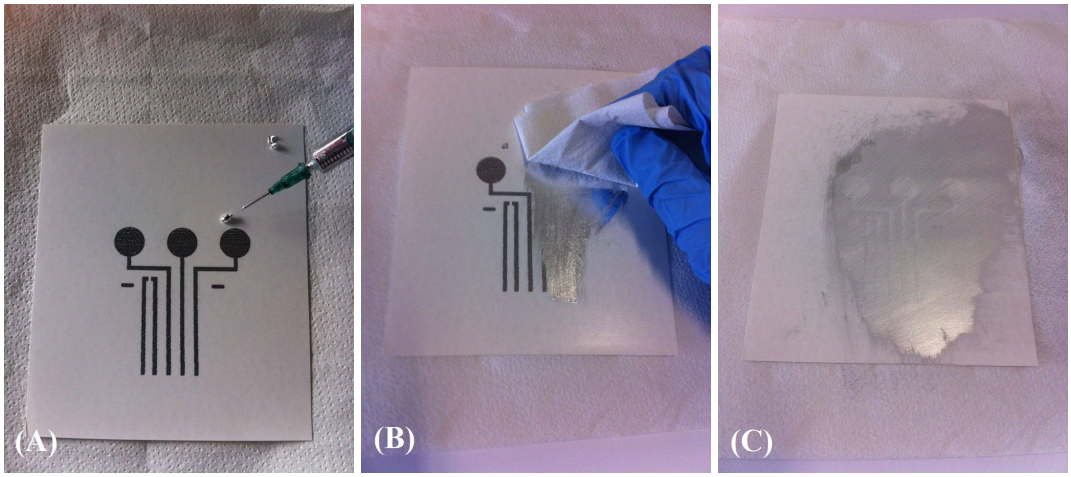

Fig. 4.3 (A) Placing drops of EGaIn LM on TTP, (B) Rubbing and applying pressure with a soft paper, (C) Final result. LM distributed over TTP.

After alloying the LM, we will now remove the LM surplus. To do this, an acetic acid solution is used. We drop the solution over the TTP and after a few seconds, the LM outside the circuit traces starts to wash away, Fig. 4.4 (A). The process is repeated until the substrate is fully clean. Fig. 4.4 (B) shows the result after the clean and drying processes are completed. The printed traces alloyed with LM have a very high conductivity now.

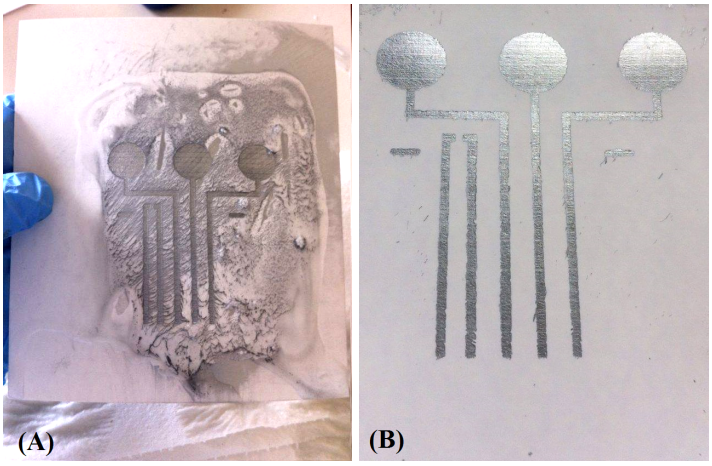

Fig. 4.4 (A) Cleaning the surplus LM over the substrate using an AAS, (B) Final result after cleaning and drying the substrate.

The red LED is then placed in a pre-defined position and fixed using CSPP. Heating the surrounding area with a heat-gun, the paste solidifies, fixing the LED in position.

After assembling the electronic components, the circuit is now ready to be transferred. Using a container filled with water, the host piece is submerged and the TTP placed in the water, floating, Fig. 4.5 (A). Passing a few seconds, the protective back layer and the TTP top film are separated, due to the reaction with water and the PVAc mid layer, Fig. 4.5 (B).

The host piece is grabbed and pulled above, catching the TTP film while doing so. The film will adhere to the surface and adapt to its shape. In this case, a 180º degrees bend is done as Fig. 4.5 (C) shows.

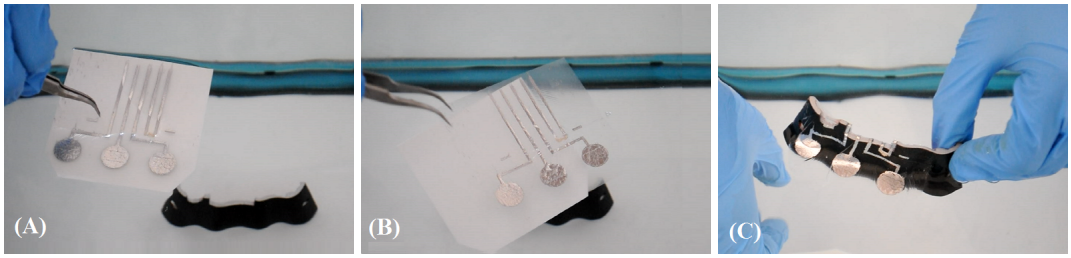

Fig. 4.5 (A) TTP with printed circuit and LED floating in the water. The host piece is submerged, (B) Protective back layer from TTP detaching, (C) Attaching the TTP film to the host piece.

After removing the host piece with the attached TTP film from the water container, we dry it until no water is found in the TTP with a heat-gun. As Fig. 4.6 shows, the final result is a fixed TTP film with conductive traces and a working electronic component.

Fig. 4.6 Final result after transferring the TTP film to the host piece, showing the front and back respectively.

To finish this prototype, we will now connect the wires before spraying the protective plastic paint over the piece. To do so, we connect one wire to each one of the circuit connections and fix it using CSPP. After a sintering process, the paste will solidify and permanently fix the wires, Fig. 4.7 (A). The wires are used to connect the bottoms to a *Cypress CY8KIT041* Board which will read the inputs from the user when a bottom is pressed. Plastic protective spray paint is now applied over the piece and let to dry for two hours. The prototype is complete and is ready to be applied in the robotic-hand.

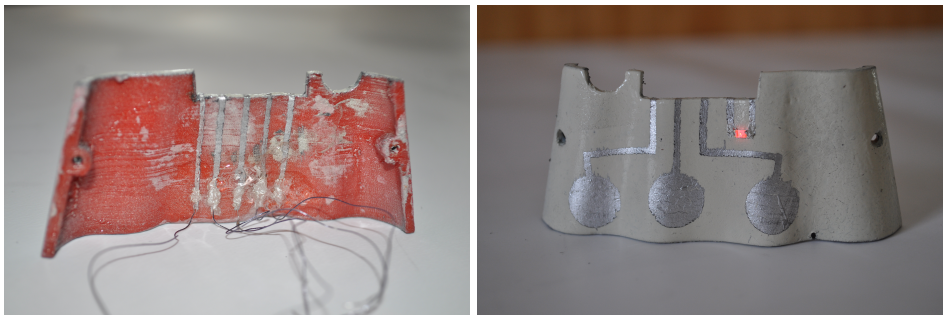

Fig. 4.7 (A) Back part of the hand piece with connected wires using CSPP, (B) Front part of the hand piece after applying the protective plastic spray.

The hand piece is now fixed in the robotic hand and using a micro-controller (*Cypress CY8KIT041* Board) we are now able to control the robotic hand. "Full-open", "full-close"

and "on/off" functions were applied to one of each bottoms. Fig. 4.8 shows the user placing the finger on the "full-close" bottom, grabbing a blue squared object.

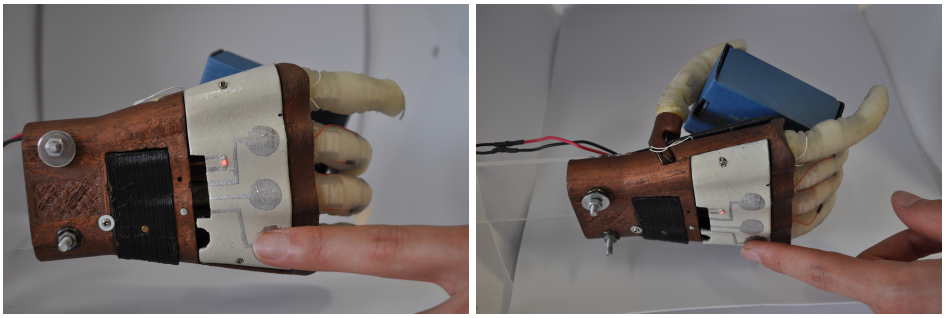

Fig. 4.8 Robotic Hand grasping an object using the capacitive bottom.

4.0.2 Capacitive Multi-Layer Keyboard

To make a functional capacitive keyboard, a switch matrix is used to output the correct characters when pressing a desired key. A keyboard switch matrix consists in horizontal lines crossing vertical lines in different layers, in a grid called circuit matrix. Each line and column is connected, via wires, to a *Cypress CY8KIT041* Board that reads each line and column as capacitive proximity sensor, Fig. 4.9.

To produce this keyboard, an initial bottom PDMS layer with 0.5*mm* was cured. The matrix columns were printed in TTP substrate, turning them conductive with LM alloy and cleaning processes. TTP printed and now conductive columns are then transferred to the cured PDMS layer. An electrical wire is connected to each one of the columns using the conductive silver polymer paste (CSPP). Another top PDMS layer is deposited and cured, with a thickness of 0.5*mm*. We now print the matrix lines in TTP, turning them conductive using the same process. These are now transferred to the previously deposited and cured PDMS top layer. The lines are connected with wires in this step. Finally, another PDMS layer with 0.5*mm* of thickness is deposited above and cured, finishing the producing process.

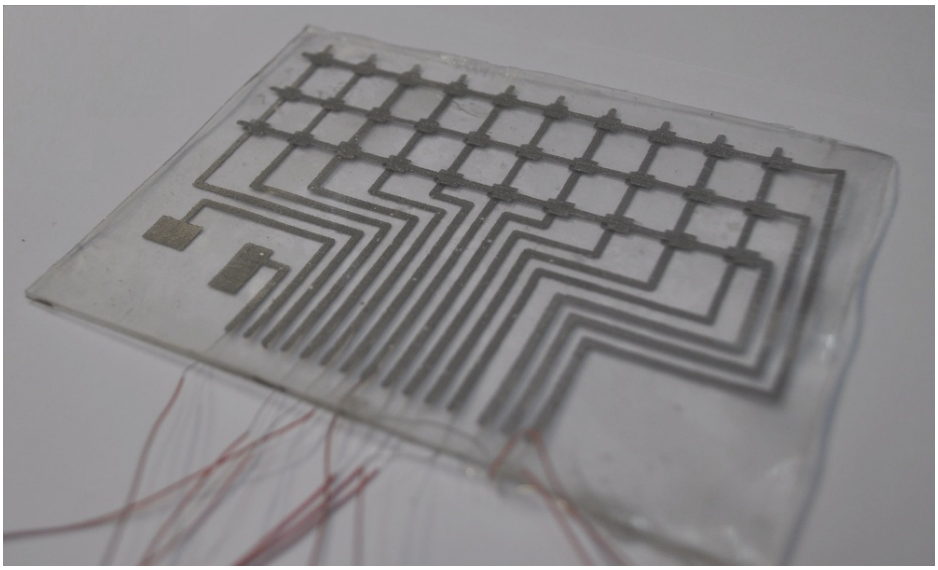

Fig. 4.9 Capacitive Keyboard with 32 intersections and 2 independent bottoms for Space and Enter.

Being a matrix, each intersection between the lines and columns will be used as a key-spot to output a desired character in the user's computer console. With a simple software development using cypress development software, we are able to read the proximity values in each line and column when a conductive object (e.g. finger) passes by. A capacitive threshold is imposed to avoid wrong or ghost readings.

When both a column and line pass that threshold the software will output the corresponding character in the intersection.

Advantages when using this type of keyboard are waterproofing, flexibility, stretchability, resistance to shock and wear and, most of all, cheap to develop and produce.

A simple improvement would be using a bluetooth micro-controller inserted in the keyboard and connected to the lines and columns to remove the need to use wires.

4.0.3 Headphone with integrated capacitive bottoms

Headphone users usually struggle to reach their pockets when performing different types of physical activities (e.g. running, jogging, gym classes). To improve the way users interact with the device like controlling the volume or turn the device "on" and "off", a prototype is developed. While many other things could be added, developing a simple prototype to prove the concept works is our main objective.

Using TTP substrate, a volume controller, with "minus" and "plus" bottoms, and "On" and "Off" bottoms will be printed on. Two independent traces are also printed to include

a red LED. These bottoms are connect to a micro-controller, *Cypress CY8KIT041* Board, which will detect the proximity of the finger. Passing the defined threshold when a bottom is press, the information is passed to the headphone's micro-controller and act as a regular bottom. The red LED will turn red while this happens for aesthetic proposes, Fig. 4.10.

Fig. 4.10 Capacitive headphone. User pressing "On" bottom to turn the device on, turning the red LED active.

The conductive bottoms are transferred to the headphone outside case. Using the 180º bending technique, the conductive traces can remain conductive while bending to the inside part, Fig. 4.11.

Fig. 4.11 Capacitive headphone bottoms with conductive traces bending to the inside part of the headphone case.

After the transferring is complete, using a transparent plastic paint spray, the circuit is sealed and protected from water, humidity and common wear. Making this prototype proved that the concept works in common gadgets as simple as a headphone, and although many more features could be added (e.g. track switcher, led light controllers for aesthetic proposes), a simple prototype to develop was chosen for now.

4.0.4 EMG Reader Tattoo

Electromyography or EMG is used to evaluate the health condition of muscle and nerves cells that control them. Those cells transmit electrical signals that cause muscles to contract and relax. These signals will be acquired by the EMG electrodes and translate them into graphs or numbers that can later be used depending the final propose, shall it be to detect muscle or nerve issues, or to control devices and movements in the technology ground.

To perform an EMG diagnosis, the electrodes used to acquire the signals must be in direct contact with the skin of the user. For better results, several electrodes are used.

Developing a way to acquire signals in a similar way those industrial produced electrodes does is no easy task. To start with, a EMG signal reader and translator device is used to understand the signals obtained. To obtain those signals, a three part electrode is required, composed by the outside square areas to read the signals and the mid square area used as ground, Fig. 4.12. After printing a similar schematic on TTP substrate with AgNP ink, alloying LM and cleaning the excess, three wires are connect to each area in the end of the conductive traces.

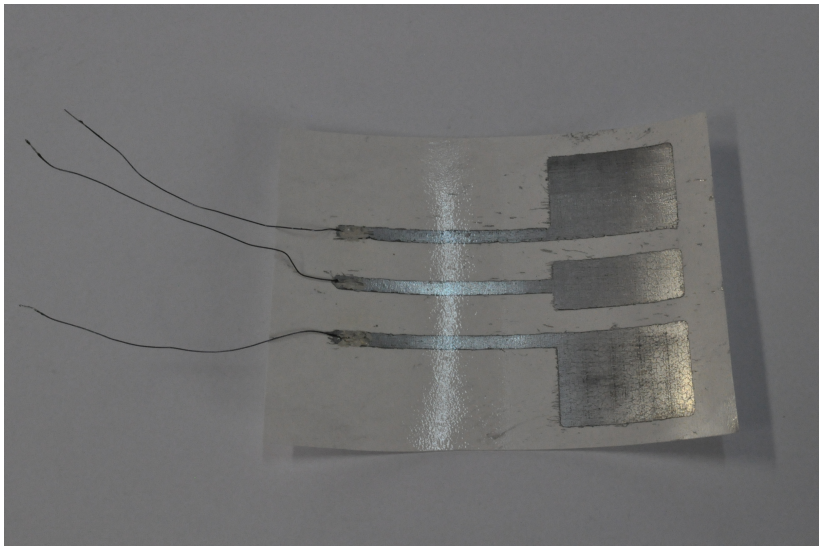

Fig. 4.12 Printed EMG electrode on TTP substrate, alloyed with LM and cleaned, with three wires attached for readings.

Only the square areas must be in contact with the skin, and for that reason, a transparent plastic spray paint is used to insulate the everything but the squares in question. That way, when transferring to the skin, false readings due to the conductive traces will not be recorded by the EMG device.

The next step is to connect the three wires in the created electrode tattoo to the EMG signal reading device simply by soldering to the respective PCB beds, Fig. 4.13.

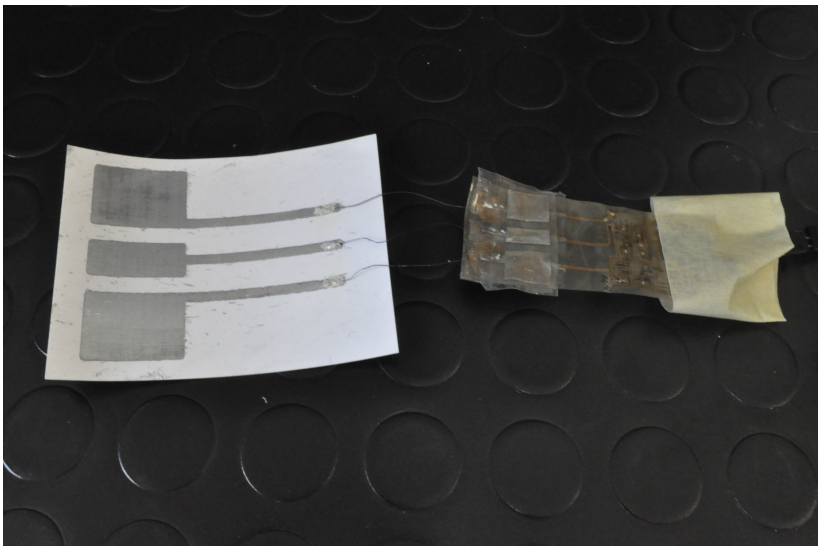

Fig. 4.13 Printed EMG electrode on TTP substrate connected to the EMG signal reading device.

Using the direct transfer method, the TTP Electrode is now placed in the skin, directly facing it. Water and pressure is then applied in the protective back layer, Fig. 4.14 (A), and after a few seconds, it is peeled off, leaving on the electrode that can be seen due to the transparency of the film, Fig. 4.14 (B). The EMG signal reader is kept in place using glue-tape.

Fig. 4.14 (A) Watering the protective back layer of the TTP, (B) Peeling off the protective back layer, leaving the electrode exposed due to the film transparency.

After all these steps are concluded, the EMG signal reader will now acquire the electrical impulses from the muscles and nerves that will be sent to another device to translate those signals into gestures. Several gestures, such as when the user open or closes the hand, can be recorded due to the software developed, Fig. 4.15.

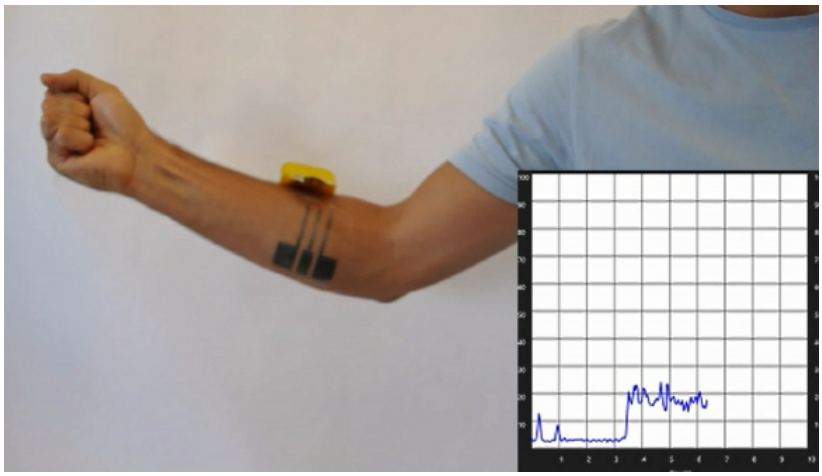

Fig. 4.15 Software recording data as hand is closed for some seconds.

Some of the issues found when developing this prototype was the data transmission, where a delay is always found between the user hand movements and the reproduced signal to the screen, which can be easily fixed with some software tweaks. Another issues is the EMG reader device being glue-taped to the skin to remain in the same position. To overcome this, a smaller micro-controller could be implemented.

Chapter 5

Future Work and Publications

5.0.1 Future Work

With the presented work, an important contribution was made for electronic skins and hydro-transfer methods. With the cases study, it is possible to apply this work and technology in many distinct research and consumer areas. Many of the initial prototypes can be improved by removing the need of external connections (e.g. wires) to processing board. Instead, a bluetooth or an wireless data transmitter can be directly applied in the prototypes. More complex circuits can be printed to carry out more and different functions on the developed prototypes. Multi-layer circuits is possible to developed with our current researches in future prototypes.

Micro-sized circuits can not be printed with the current printing method, so a direct laser patterning method can be investigated to accomplish this objective. This will open doors to more complex electronic tattoos, like an heat-harvester or sweat analyser, using the technology researched in this dissertation.

Different approaches as new types of nano particle inks and stretchable substrates can be tested to get similar or better results. Direct material printing over TTP using specialized printers can prove to have very good end results, although being a very expensive processes.

Mastering and improving the hydro-transfer method with the right substrate can be done using specialized tools and bigger containers researched for this propose.

A more extensive SEM analyses can help conclude some of our remaining questions about certain reactions between the different particles.

5.0.2 Publications

The work developed in this dissertation resulted in the following publications:

- **Prepared**:

  1. Hydrographics Electronics through e-Gain Activated Silver Ink: Functionalize any 3D surface M. Tavakoli, Hugo Paisana, Anibal T. de Almeida, Carmel Majidi.

- **Patent**:

  1. Mahmoud Tavakoli, Hugo Paisana, Anibal de Almeida, Carmel Majidi, "Fabrication method and material composition for Electronic Tattoos", Provisional US Patent Submitted, 2017.

References

[1] B. Meinhold, "Smarty Ring Lets You Control Your Smartphone Without Lifting a Finger," 2013.

[2] Statista, "Forecasted value of the global wearable devices market from 2012 to 2018," 2011.

[3] H. Z. Xiandi Wang, Lin Dong, "Recent progress in electronic skin," *Advanced Science*, 2015.

[4] Y. X. Ahyeon Koh, Daeshik Kang, "A soft, wearable microfluidic device for the capture, storage, and colorimetric sensing of sweat," *Science Translational Medicine*, 2016.

[5] M. P. Mills, "Silver Nano Ink," 2013.

[6] X. Tao, *Wearable Electronics and Photonics*. Woodhead Publishing Ltd and CRC Press LLC, 2005.

[7] Y. A. Garnier F, Hajlaoui R, "All-polymer field-effect transistor realized by printing techniques," *Science*, 1994.

[8] D. A. Bao ZN, Feng Y, "High-performance plastic transistors fabricated by printing techniques," *Chem Mater*, 1997.

[9] M. A. Reuss RH, Chalamala BR, "Macroelectronics: perspectives on technology and applications," *Proc IEEE*, 2005.

[10] B. K. Rogers JA, Bao Z, "Paper-like electronic displays: large-area rubberstamped plastic sheets of electronics and microencapsulated electrophoretic inks.," *Proc Natl Acad Sci USA*, 2001.

[11] V. V. E. Gelinck GH, Huitema HEA, "Flexible activematrix displays and shift registers based on solutionprocessed organic transistors.," *Nat Mater*, 2004.

[12] H. Y. Rogers JA, Someya T, "Materials and mechanics for stretchable electronics.," *Science*, 2010.

[13] M. R. Kim DH, Lu NS, "Epidermal electronics.," *Science*, 2011.

[14] L. Y. Huang X, Yeo WH, "Epidermal differential impedance sensor for conformal skin hydration monitoring.," *Biointerphases*, 2012.

[15] A. J. Kim DH, Viventi J, "Dissolvable films of silk fibroin for ultrathin conformal bio-integrated electronics.," *Nat Mater*, 2010.

[16] L. N. Kim DH, Ghaffari R, "Electronic sensor and actuator webs for large-area complex geometry cardiac mapping and therapy.," *Proc Natl Acad Sci USA*, 2012.

[17] K. H. Kim DH, Wang SD, "Thin, flexible sensors and actuators as "iinstrumented" surgical sutures for targeted wound monitoring and therapy.," *Small*, 2012.

[18] K. Hoffman, "Electronic skin," *University of Rhode Island BME 281 Second Presentation*, 2013.

[19] Americaninno, "The Rehab Institute of Chicago Tests Its Revolutionary Thought-Controlled Bionic Leg," 2015.

[20] T. Construct, "Wearable Technology 2017-2027: Markets, Players, Forecasts," 2017.

[21] Markets and M. Ltd, "Stretchable Electronics Market - Trends and Forecast to 2015-2023," 2014.

[22] P. Intelligence, "Archive for the "MEMS" Category," 2016.

[23] H. Z. James Hayward, Guillaume Chansin, *Wearable Technology 2017-2027: Markets, Players, Forecasts*. IDTechEx, 2017.

[24] D.-H. K. Nanshu Lu, "Flexible and stretchable electronics paving the way for soft robotics," *Soft Robotics*, 2013.

[25] D.-H. Kim, N. Lu, R. Ma, Y.-S. Kim, R.-H. Kim, S. Wang, J. Wu, S. M. Won, H. Tao, A. Islam, *et al.*, "Epidermal electronics," *science*, vol. 333, no. 6044, pp. 838–843, 2011.

[26] M. Kaltenbrunner, T. Sekitani, J. Reeder, T. Yokota, K. Kuribara, T. Tokuhara, M. Drack, R. Schwödiauer, I. Graz, S. Bauer-Gogonea, *et al.*, "An ultra-lightweight design for imperceptible plastic electronics," *Nature*, vol. 499, no. 7459, p. 458, 2013.

[27] D.-Y. Wang, Y. Chang, Q.-S. Lu, and Z.-G. Yang, "Nano-organic silver composite conductive ink for flexible printed circuits," *Materials Technology: Advanced Performance Materials*, vol. 30, 2015.

[28] H.-L. C. Kao, C. Holz, A. Roseway, A. Calvo, and C. Schmandt, "Duoskin: rapidly prototyping on-skin user interfaces using skin-friendly materials," in *Proceedings of the 2016 ACM International Symposium on Wearable Computers*, pp. 16–23, ACM, 2016.

[29] L. Bareket, L. Inzelberg, D. Rand, M. David-Pur, D. Rabinovich, B. Brandes, and Y. Hanein, "Temporary-tattoo for long-term high fidelity biopotential recordings," *Scientific reports*, vol. 6, p. 25727, 2016.

[30] M. Weigel, A. S. Nittala, A. Olwal, and J. Steimle, "Skinmarks: Enabling interactions on body landmarks using conformal skin electronics," in *Proceedings of the 2017 CHI Conference on Human Factors in Computing Systems*, pp. 3095–3105, ACM, 2017.

[31] N. Matsuhisa, M. Kaltenbrunner, T. Yokota, H. Jinno, K. Kuribara, T. Sekitani, and T. Someya, "Printable elastic conductors with a high conductivity for electronic textile applications," *Nature communications*, vol. 6, 2015.

[32] N. Matsuhisa, D. Inoue, P. Zalar, H. Jin, Y. Matsuba, A. Itoh, T. Yokota, D. Hashizume, and T. Someya, "Printable elastic conductors by in situ formation of silver nanoparticles from silver flakes," *Nature Materials*, 2017.

[33] M. T. Review, "Stick-On Electronic Tattoos," 2011.

[34] D. M. Ta Saponas, Da Tan, "Enabling always-available input with muscle computer interfaces," *UIST09*, 2010.

[35] F. Sullivan, "Electronic Skin - Advancements and Emerging Opportunities," 2016.

[36] G. W. K. Xian Huang, Yuhao Liu, "Epidermal radio frequency electronics for wireless power transfer," *Nature*, 2016.

[37] R. C. W. Limei Tian, Yuhang Li, "Flexible and stretchable 3w sensors for thermal characterization of human skin," *Advanced Functional Materials*, 2017.

[38] S. Alessandra Zucca, Christian Cipriani, "Tattoo conductive polymer nanosheets for skin-contact applications," *Materials Views*, 2016.

[39] I. M. La Tchvialeva, Ha Zeng, "Skin roughness assessment," *New Developments in Biomedcial Engineering*, 2014.

[40] R. M. Da Kim, Ha Lu, "Epidermal electronics," *Science 333*, 2011.

[41] A. Bandodkar, "Tattoo-based noninvasive glucose monitoring," *Analytical Chemistry*, 2015.

[42] G. O. D. Kang, Y. S. Kim, "Scalable microfabrication procedures for adhesive-integrated flexible electronic sensors," *Sensors*, 2015.

[43] N. W. Joanne Lo, Doris Jung-Lin Lee, "Skintillates: Designing and creating epidermal interactions," University of California, Berkeley, 2017.

[44] M. S. S. Karsten Bleech, *3D Polymer Printing with Desktop Inkjet Technology*. PhD thesis, WorcesterR Polytechnic Institute, 2009.

[45] J. L. Aaron Costello, *Report for a major qualifying project*. PhD thesis, WorcesterR Polytechnic Institute, 2010.

[46] HP, "HP 60 Inkjet Cartridge," 2009.

[47] J. J. S.B. Fuller, E.J. Wilhelm, "Ink-jet printed nanoparticle microelectromechanical systems," *Microelectromechanical Systems*, 2002.

[48] Y. L. Daeyoung Kim, Jun Hyeon Yoo, *Gallium-Based Liquid Metal Inkjet Printing*. PhD thesis, The University of Texas at Dallas, 2016.

[49] Silhouette, "Silhouette Temporary Tattoo Paper," 2012.

[50] E. Britannica, "Polyvinyl acetate (PVAc)," 2008.

[51] E. TXIB, "Non-phthalate plasticizer for polyvinyl acetate (PVAc) emulsion adhesives in woodworking and bookbinding," 2009.

[52] D. Lide, "Crc handbook of chemistry and physics," 2007.

[53] J. L. X. Wang, "Recent advancements in liquid metal flexible printed electronics: Properties, technologies, and applications," *Multidisciplinary Digital Publishing Institute*, 2016.

[54] C. M. J. Wissman, T. Lu, "Soft-matter electronics with stencil lithography," *Sensors IEEE*, 2013.

[55] C. M. T. Lu, L. Finkenauer, "Rapid prototyping for soft-matter electronics," advanced functional materials," *Advanced Functional Materials*, 2014.

[56] C. M. A. Tabatabai, A. Fassler, "Liquid-phase gallium–indium alloy electronics with microcontact printing," *Langmuir*, 2013.

[57] L. O. M. Tavakoli, R. Rocha, "Carbon doped pdms: conductance stability over time and implications for additive manufacturing of stretchable electronics," *Journal of Micromechanics and Microengineering*, 2017.

[58] E. L. W. R. K. Kramer, J. William, "Mechanically sintered gallium-indium nanoparticles," *CTUM*, 2015.

[59] M. D. D. C. B. Eaker, D. Hight, "Oxidation-mediated fingering in liquid metals," *Cornell University Library*, 2017.

[60] S. Swapp, "Scanning Electron Microscopy (SEM)," 2010.